

Review

Recent Advances on Iron(III) Selective Fluorescent Probes with Possible Applications in Bioimaging

Suban K. Sahoo ^{1,*}  and Guido Crisponi ² ¹ Department of Applied Chemistry, S.V. National Institute Technology, Surat 395007, Gujrat, India² Dipartimento di Scienze Chimiche e Geologiche, Università di Cagliari, 09042 Monserrato, Italy; crisponi@unica.it

* Correspondence: suban_sahoo@rediffmail.com

Academic Editor: Valeria M Nurchi

Received: 18 August 2019; Accepted: 6 September 2019; Published: 7 September 2019



Abstract: Iron(III) is well-known to play a vital role in a variety of metabolic processes in almost all living systems, including the human body. However, the excess or deficiency of Fe³⁺ from the normal permissible limit can cause serious health problems. Therefore, novel analytical methods are developed for the simple, direct, and cost-effective monitoring of Fe³⁺ concentration in various environmental and biological samples. Because of the high selectivity and sensitivity, fast response time, and simplicity, the fluorescent-based molecular probes have been developed extensively in the past few decades to detect Fe³⁺. This review was narrated to summarize the Fe³⁺-selective fluorescent probes that show fluorescence enhancement (turn-on) and ratiometric response. The Fe³⁺ sensing ability, mechanisms along with the analytical novelties of recently reported 77 fluorescent probes are discussed.

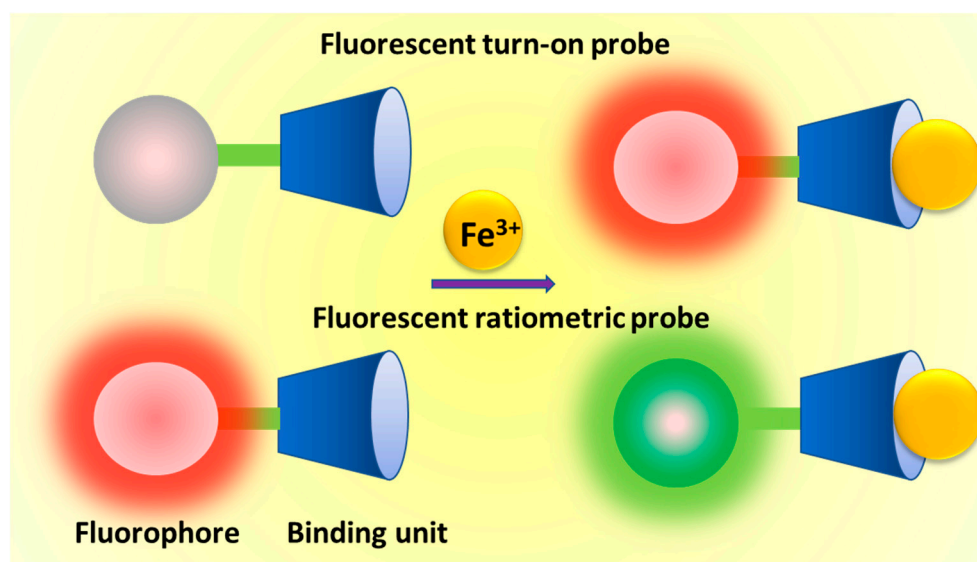
Keywords: Fluorescent sensors; Turn-on sensors; Ratiometric sensor; iron(III); Bioimaging

1. Introduction

Iron is well known to play an important role in a variety of physiological processes in the human body, such as oxygen metabolism, muscle contraction, synthesis of DNA and RNA, nerve conduction, proton transfer, enzyme synthesis, and regulation of acid-base balance and osmotic pressure in cells [1]. Despite the biological importance, the excess (hyperferremia) and the deficiency (hypoferremia) of iron can lead to serious health problems. The iron overload in the human body can cause severe diseases like osteoporosis, cancers, dysfunction of organs, hemochromatosis, and Alzheimer's and Parkinson's disease [2], whereas the iron deficiency can cause anemia and affect several cellular metabolic processes [3]. During the iron disorder, the labile iron generates destructive oxygen species (such as hydroxyl radical) via the Fenton reaction due to the facile redox process between Fe²⁺ and Fe³⁺ in the presence of molecular oxygen. The reactive oxygen species can damage peroxidative tissue and cause serious complications in pathological situations like β -thalassemia [4]. Therefore, there is a need for novel analytical methods for the monitoring of iron concentration in various environmental, industrial, and biological samples.

The optically (chromogenic and fluorogenic) active molecular probes have been widely investigated for the selective detection of Fe³⁺ in the last few decades. Among the two optical modes, the fluorescence-based molecular probes are extensively developed because of their simplicity, high selectivity and sensitivity, precise and real-time measuring of the target analyte up to a very low concentration without the need of pre-treatment of the sample, and sophisticated instrument [5]. The fluorescent probes are mainly designed by suitably connecting the chelating agent (binding unit) with a light-emitting group (fluorophore unit) (Scheme 1). The selective complexation of target analyte with the binding unit alters the fluorescence property of the photoexcited fluorophore mainly due to the

energy or electron transfer, which allows quantifying the target analyte. The fluorescence signals from the probe upon analyte binding can be observed in the form of enhancement (turn-on), quenching (turn-off), or red/blue-shift in the fluorescence maxima of the probe (ratiometric). The well-known mechanisms like fluorescence resonance energy transfer (FRET), photo-induced electron transfer (PET), intramolecular charge transfer (ICT), C=N isomerization, chelation-induced enhanced fluorescence (CHEF), excimer formation, etc. have been applied to develop fluorescent probes for the selective detection of various analytes, including Fe^{3+} , and the mechanisms are well described in the recently published review paper [6].



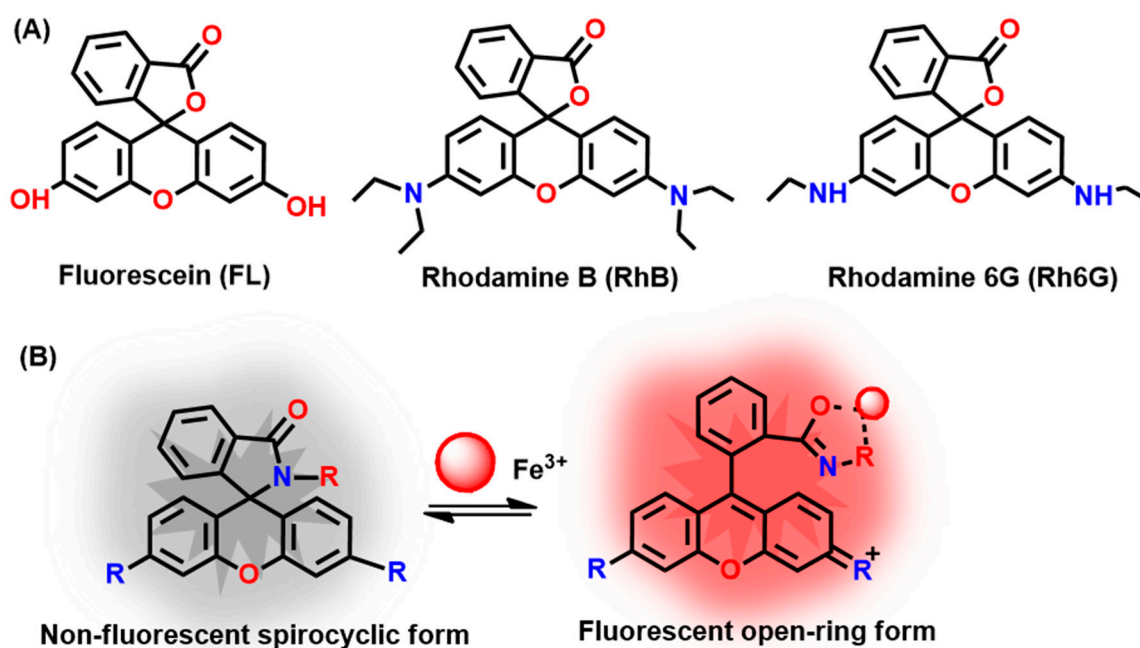
Scheme 1. Schematic illustration of the components and signaling of fluorescent turn-on and ratiometric probes.

In 2012, we reviewed the various molecular and supramolecular fluorescent probes developed for the selective detection of Fe^{3+} [7] and observed that most of the fluorescent probes are based on the fluorescent quenching mechanism due to the paramagnetic nature of Fe^{3+} [8,9]. The fluorescent turn-on and ratiometric probes possess several analytical novelties like less probability to give false signals, increased sensitivity over turn-off probes, and, therefore, several Fe^{3+} -selective fluorescent turn-on and ratiometric probes are reported in the last few years. This critical review was narrated to summarize the Fe^{3+} -selective fluorescent turn-on and ratiometric probes developed after 2012, and discussion has been made on the sensing mechanisms with their potential applications to biological samples for the qualitative and quantitative monitoring of intracellular Fe^{3+} ions in live cells. All the fluorescent probes were presented in three different groups: (i) fluorescent turn-on probes for Fe(III), (ii) fluorescent ratiometric probes for Fe(III), and (iii) fluorescent chemodosimeters for Fe(III) according to their signaling process and sensing mechanisms.

2. Fluorescent Turn-on Probes for Fe(III)

The paramagnetic nature of the Fe^{3+} is well known to quench the fluorescence from the organic fluorophores and, therefore, the majority of the reported Fe^{3+} -selective fluorescent probes show fluorescent turn-off responses. Also, it is challenging to develop fluorescent probes for an iron that showed turn-on and/or ratiometric fluorescent responses. The fluorescent probes with the turn-on response have several analytical advantages like high sensitivity, low background, and their potential applications in live-cell imaging. The literature survey revealed that the rhodamine/fluorescein derivatives are extensively applied for the development of fluorescent turn-on probes for various ionic and neutral analytes because of the reversible fluorescence changes with respect to the structural

changes occurred in the spirocyclic ring [10]. The closed ring spirocyclic form of the rhodamine is colorless and non-fluorescent, while the open-ring spirocyclic form is highly fluorescent and colored. The general mechanism to design rhodamine/fluorescein-based fluorescent turn-on probes for Fe^{3+} is described in Scheme 2. The carboxyl frame of rhodamine is converted into a closed ring form by reacting with small molecules possessing $-\text{NH}_2$ group, and then the complexation-induced opening of the spirocyclic ring results in strong fluorescence emission. With this mechanism, the recently developed rhodamine-based Fe^{3+} -selective fluorescent probes 1–40 are summarized in Table 1.



Scheme 2. (A) The structure of fluorescein, rhodamine B, and rhodamine 6G; (B) The general schematic representation of the mechanism of complexation-induced opening of the spirocyclic ring to give fluorescent enhancement in rhodamine-based fluorescent turn-on probes.

Table 1. Fe³⁺-selective rhodamine/fluorescein-based fluorescent turn-on probes.

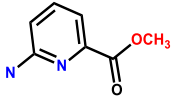
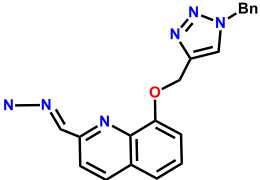
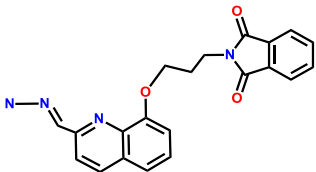
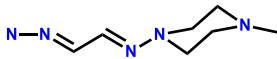
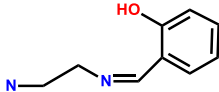
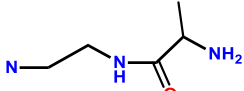
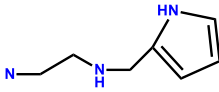
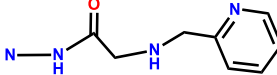
| Probes | Rh/FL | Rh/FL-Y | Medium | Ex./Em. λ (nm) | LOD | Cells Imaging | Ref. |
|--------|-------|---|---|------------------------|---------------|-------------------------------|------|
| 1 | RhB |  | CH ₃ CN/Tris-HCl buffer (pH 7.3, 2:1, v/v) | 510/580 | 0.1 μ M | Human SH-SY5Y | [11] |
| 2 | Rh6G |  | Tris HCl-CH ₃ CN (1:1, v/v, pH 7.4) | 510/552 | 50 nM | Fibroblast | [12] |
| 3 | Rh6G |  | EtOH-H ₂ O (3:7, v/v) | 505/559 | - | EJ (cysticcancer) | [13] |
| 4 | RhB |  | H ₂ O-MeOH (v/v = 9:1, Tris-HCl, pH = 7.4) | 564/588 | 2.2 μ M | HeLa | [14] |
| 5 | RhB |  | MeOH-H ₂ O (1:1, v/v, Tris-HCl, pH = 7) | 520/582 | - | B16-F10 murine melanoma cells | [15] |
| 6 | RhB |  | H ₂ O-MeOH (60:40, v/v) at pH 7 | -/599 | 3 μ M | L-929 | [16] |
| 7 | RhB |  | MeOH/H ₂ O (3:2, v/v, pH 7.10, HEPES buffer) | 558/581 | 0.031 μ M | Human liver cells (L-02) | [17] |
| 8 | RhB |  | MeOH/H ₂ O (1/99) buffer (pH 7, 20 mM HEPES, 50 mM NaNO ₃) | 530/586 | - | 7402 cells | [18] |

Table 1. Cont.

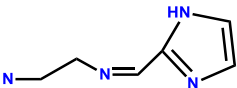
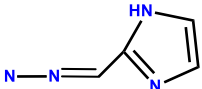
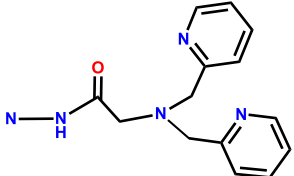
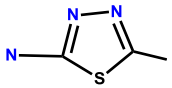
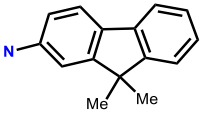
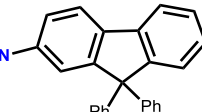
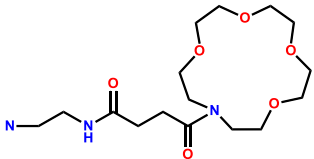
| Probes | Rh/FL | Rh/FL-Y | Medium | Ex./Em. λ (nm) | LOD | Cells Imaging | Ref. |
|--------|-------|---|---|------------------------|---------------|-------------------------------|------|
| 9 | Rh6G |  | DMSO/H ₂ O (2:8, 50 mM PBS buffered, pH = 7.4) | 480/553 | 66 nM | Candida albicans cells | [19] |
| 10 | Rh6G |  | DMSO/H ₂ O (2:8, 50 mM PBS buffered, pH = 7.4) | 480/553 | 44.5 nM | Candida albicans cells | [19] |
| 11 | RhB |  | MeOH/H ₂ O (1/99) buffer (pH 7, 20 mM HEPES, 50 mM NaNO ₃) | 530/586 | - | 293FT cells | [20] |
| 12 | RhB |  | MeOH/H ₂ O (1:1, v/v) | 555/584 | 0.32 μ M | HepG2 (liver cells) | [21] |
| 13 | RhB |  | EtOH-H ₂ O (5:5, v/v, PBS, pH = 7.4) | 530/583 | 0.9 μ M | L929 cells | [22] |
| 14 | RhB |  | EtOH-H ₂ O (5:5, v/v, PBS pH = 7.4) | 530/583 | 5 μ M | L929 cells | [22] |
| 15 | RhB |  | MeOH/H ₂ O (1:1, v/v, pH = 7.4) | 558/581 | 0.396 μ M | Neuronal cell line PC12 cells | [23] |

Table 1. Cont.

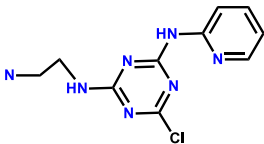
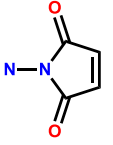
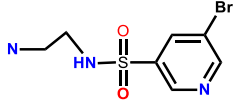
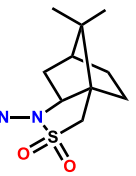
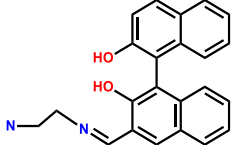
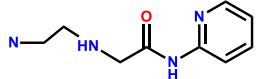
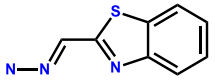
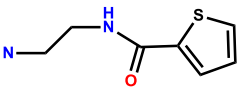
| Probes | Rh/FL | Rh/FL-Y | Medium | Ex./Em. λ (nm) | LOD | Cells Imaging | Ref. |
|--------|-------|---|--|------------------------|--------------|----------------|------|
| 16 | RhB |  | H ₂ O | 520/582 | 41 nM | HL-7702 cells | [24] |
| 17 | RhB |  | EtOH-H ₂ O (4/1, v/v, pH 7) | 455/581 | - | Hela | [25] |
| 18 | RhB |  | CH ₃ OH, H ₂ O (3/7, Tris-HCl buffer, pH = 7.40) | 535/579 | 3.49 μ M | MGC-803 cells | [26] |
| 19 | RhB |  | (1: 1 = H ₂ O: CH ₃ CN, v/v) | 540/580 | 0.26 μ M | NPC-C666 cells | [27] |
| 20 | RhB |  | HEPES buffer, pH = 7, THF/H ₂ O 3/7, v/v | 510/585 | 183 nM | HeLa | [28] |
| 21 | RhB |  | MeOH/H ₂ O (1:1, v/v) | 500/560 | 57 nM | A549 cells | [29] |
| 22 | FL |  | DMSO/H ₂ O (3:7/v/v) HEPES buffered pH 7.2 | 393/515 | 7.4 nM | Hep G2 cells | [30] |
| 23 | Rh6G |  | C ₂ H ₅ OH/H ₂ O (1:1, v/v) | 510/555 | 6 μ M | HeLa | [31] |

Table 1. Cont.

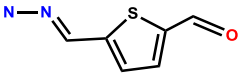
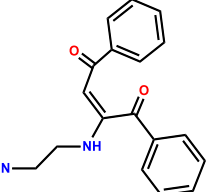
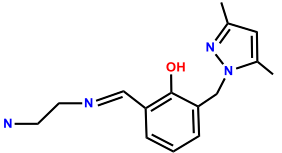
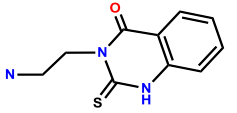
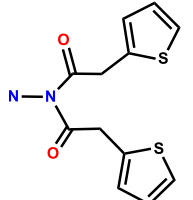
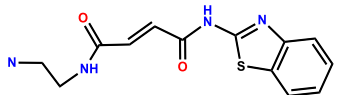
| Probes | Rh/FL | Rh/FL-Y | Medium | Ex./Em. λ (nm) | LOD | Cells Imaging | Ref. |
|--------|-------|---|--|------------------------|---------------|----------------|------|
| 24 | RhB |  | EtOH-H ₂ O, 6:4(v:v), Ph = 7.2, HEPES buffer | 450/582 | 17 nM | DL tumor cells | [32] |
| 25 | RhB |  | EtOH/H ₂ O (9:1, v/v; HEPES buffer, pH = 7.2) | 510/588 | 0.768 μ M | HeLa | [33] |
| 26 | Rh6G |  | MeOH/H ₂ O (1:1, v/v, pH 7.2, 40 mM HEPES buffer) | 510/555 | 0.29 μ M | HepG2 | [34] |
| 27 | Rh6G |  | CH ₃ CN/HEPES (10 mM, pH = 7.40, 8/2, v/v) | 495/555 | 4.11 μ M | U251 cells | [35] |
| 28 | RhB |  | EtOH-H ₂ O (1:4) | 540/580 | 0.13 μ M | HeLa | [36] |
| 29 | RhB |  | Tris-HCl (1 mM, pH = 7.4) | 562/584 | 11.6 nM | HepG2 cells | [37] |

Table 1. Cont.

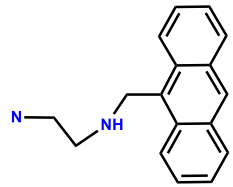
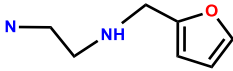
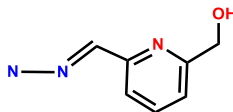
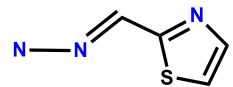
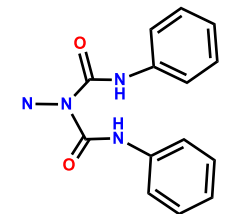
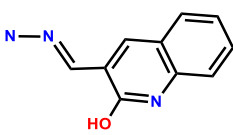
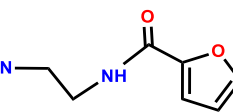
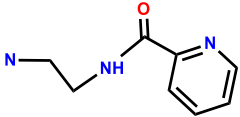
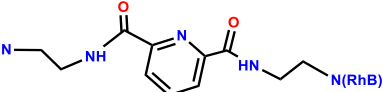
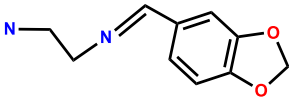
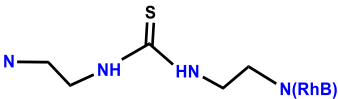
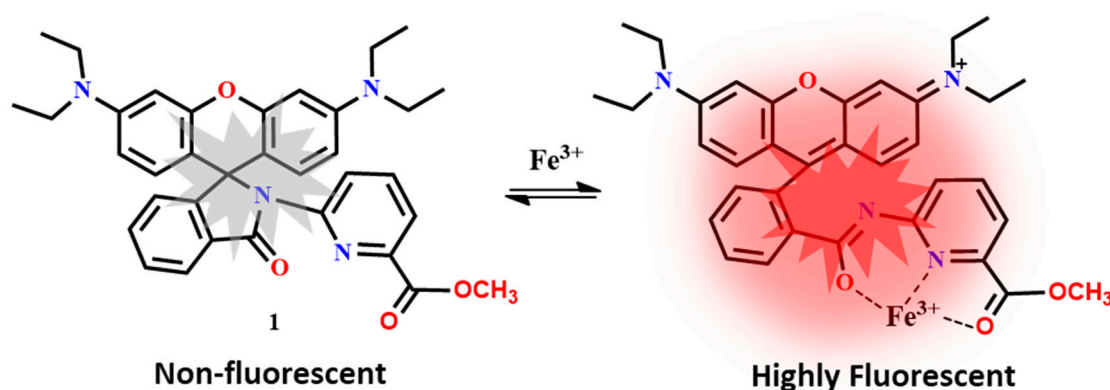
| Probes | Rh/FL | Rh/FL-Y | Medium | Ex./Em. λ (nm) | LOD | Cells Imaging | Ref. |
|--------|-------|---|--|------------------------|---------------|---------------------------------|------|
| 30 | RhB |  | EtOH/Tris-HCl buffer (v/v, 1/9, pH = 7) | 560/582 | 42 nM | HeLa | [38] |
| 31 | RhB |  | EtOH/H ₂ O (1:1, v/v) | 560/582 | 0.025 μ M | HeLa | [39] |
| 32 | RhB |  | CH ₃ CN/Tris-HCl buffer (10 mM, pH 7.3, v/v, 2:1) | 535/583 | - | Bovine aortic endothelial cells | [40] |
| 33 | RhB |  | HEPES buffer (1 mM, pH 7) | 560/596 | 92 nM | Human colon cancer cells SW480 | [41] |
| 34 | Rh6G |  | H ₂ O (containing 1% DMSO as a co-solvent) | 500/556 | 1.2 μ M | HeLa | [42] |
| 35 | Rh6G |  | H ₂ O | 510/572 | 33 nM | Zebra fish embryos | [43] |
| 36 | RhB |  | MeOH/H ₂ O (1:1, v/v, pH 7.36, HEPES buffer) | 560/582 | 0.437 μ M | MCF-7 cells | [44] |

Table 1. Cont.

| Probes | Rh/FL | Rh/FL-Y | Medium | Ex./Em. λ (nm) | LOD | Cells Imaging | Ref. |
|--------|-------|---|---|------------------------|---------------|-------------------------|------|
| 37 | RhB |  | EtOH/H ₂ O (3:1, <i>v/v</i> , HEPES, pH = 7.33) | 560/582 | 0.067 μ M | MCF-7 cells | [45] |
| 38 | RhB |  | EtOH/H ₂ O (3:1, <i>v/v</i> , HEPES, pH = 7.33) | 560/582 | 0.345 μ M | MCF-7 cells | [45] |
| 39 | RhB |  | EtOH/H ₂ O (<i>v/v</i> , 3/2) | 550/580 | 11.8 nM | SGC7901 (stomach cells) | [46] |
| 40 | RhB |  | EtOH/H ₂ O (2:1, <i>v/v</i> , HEPES buffer, pH 7.20) | 558/582 | 0.205 μ M | HeLa | [47] |

The summarized rhodamine-based probes in Table 1 detect Fe^{3+} either in aqueous or semi-aqueous medium, as well as within live cells by forming complex either in 1:1 or 1:2 ratio followed by the opening of the spirocyclic ring of the probes. The mechanism of sensing for all the probes is similar, as described in Scheme 2. The reversible fluorescent probe 1 forms complex with Fe^{3+} in 1:1 binding stoichiometry and opens the spirocyclic ring (Scheme 3), which allows to detect Fe^{3+} down to 0.1 μM [11]. This probe shows stable fluorescence over pH 3.5–8.2. The probe shows promising results to locate the intracellular Fe^{3+} ions in live SH-SY5Y cells in real-time. Also, the probe has been applied to detect the labile Fe^{3+} pools in mitochondria and endosomes/lysosomes of SH-SY5Y cells (Figure 1). The probe 2 has been applied to detect Fe^{3+} down to 50 nM and non-cytotoxic up to 6 μM [12]. Because of its high specificity from amino acids, BSA protein, and human blood serum, the probe 2 is useful in monitoring intracellular Fe^{3+} ions concentration. The probe 3 with a quinoline moiety bound to rhodamine 6G hydrazide shows good cell permeability and the ability to locate the subcellular distribution of Fe^{3+} in EJ (lung cancer) cells by fluorescence imaging experiments [13]. The probe 4 detects Fe^{3+} concentration down to 2.2 μM and is suitable between the pH 6–7.5 [14]. This cell-permeable probe has been applied to image intracellular Fe^{3+} ions in HeLa cells. The probe 5 shows permeability of the plasma membrane to rhodanal and potential to locate the iron pools in the cells [15]. The probe 6 can detect Fe^{3+} over wide pH ranges from 5 to 11 with the minimum detection limit estimated down to 3 μM [16]. Probe 6 has been applied for bioimaging experiments in L-929 cells (mouse fibroblast cells) and BHK-21 (hamster kidney fibroblast), revealing good biocompatibility, cell permeability, and minimum toxicity.



Scheme 3. Proposed binding mode of 1 with Fe^{3+} and the opening of the spirocyclic ring.

The probe 7 selectively forms a complex with Fe^{3+} in 1:1 stoichiometry and opens the spirocyclic ring to give significant fluorescence turn-on response [17]. Probe 7 can detect Fe^{3+} down to 0.031 μM , and the in situ generated 7- Fe^{3+} complex has been applied for the selective sensing of S^{2-} anions. The probe 8 is useful in detecting Fe^{3+} in the biologically relevant pH from 6 to 9 and has shown very low cytotoxicity [18]. A confocal fluorescence imaging study of 8 reveals good cell permeability and the ability to monitor intracellular Fe^{3+} in live cells. The probes 9 and 10 show similar high selectivity towards Fe^{3+} with the detection limit down to 66 nM and 44.5 nM, respectively [19]. The probe 11 bearing the di-2-picolylamine as a binding unit shows high selectivity towards Fe^{3+} , eliminates the Cr^{3+} interference during Fe^{3+} detection, and the selectivity is maintained over the pH range 6 to 7.5 [20]. The Fe^{3+} -selective probe 12 shows good linear fluorescence response from 2 μM to 20 μM with the limit of detection (LOD) estimated down to 0.32 μM [21]. The probes 13 and 14 show linearity range from 0.9–20 μM and 5–20 μM with the detection limit down to 0.9 μM and 5 μM , respectively [22]. The probe 15 alone is not-fluorescent above pH = 6, but the selective complexation with Fe^{3+} opens the spirocyclic ring to give significant turn-on fluorescence at 581 nm [23]. The probe 15 can detect Fe^{3+} down to 0.396 μM and is applied successfully for detecting Fe^{3+} in human liver cells (L-02) and rat neuronal (PC12) cells.

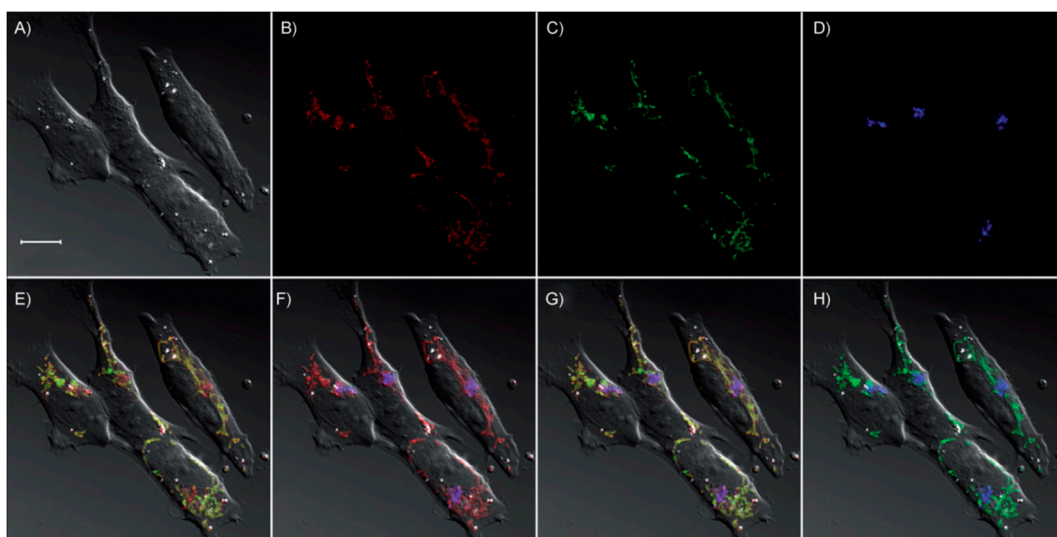


Figure 1. Representative confocal images of intracellular colocalization studies of probe **1** (10 μM) incubated with live human SH-SY5Y cells co-stained with Mito-Tracker Green (100 nM) and LysoTracker Blue DND-22 (50 nM). (A) Differential interference contrast (DIC) image of cells. (B) 1-Fe^{3+} fluorescence collected at 547–703 nm (red). (C) MitoTracker fluorescence collected at 492–548 nm (green). (D) LysoTracker fluorescence collected at 409–484 nm (blue). (E) DIC image of (A) and fluorescence images of (B,C) were merged. Colocalization regions are in yellow, and non-overlapping regions remain in the red. (F) DIC image of (A) and fluorescence images of (B,D) were merged. Overlapping regions are in purple, and non-overlapping regions remain in the red. (G) Images of (A–D) were merged, revealing that the 1-Fe^{3+} images are 100% colocalized with the sum of those of MitoTracker and LysoTracker. (H) Images of (A,C,D) were merged, showing no overlapping region between lysosomes and mitochondria. Scale bar = 10 μm (Reproduced from Ref. [11] with permission from Wiley).

The rhodamine-triazine aminopyridine derivative **16** shows the detection limit of 41 nM for Fe^{3+} , and the probe has been applied to monitor Fe^{3+} ions in real water samples and living HL-7702 cells [24]. The probe **17** is applied for the cascade detection of Fe^{3+} and the thiols (glutathione, homocysteine, cysteine) in solution and live cells [25]. The reversible fluorescent probe **18** shows turn-on fluorescence response between 10 and 70 μM of Fe^{3+} with the detection limit of 0.195 ppm [26]. The probe **19** is suitable to detect Fe^{3+} in the pH range from 4 to 7, with the estimated LOD of 0.26 μM [27]. The fluorescent enantiomer **20** shows a detection limit of 183 nM Fe^{3+} and detects Fe^{3+} in living cells with low cytotoxicity [28]. The probe **21** is ideal for detecting Fe^{3+} in the pH range from 4 to 8, with the LOD of 57 nM [29]. Also, the fluorescence turn-on response from the 21-Fe^{3+} complex formed in solution is shown to reverse upon addition of $\text{Na}_4\text{P}_2\text{O}_7$. The benzothiazole-functionalized fluorescein derivative **22** shows nanomolar detection limit (7.4 nM) for Fe^{3+} with the potential to detect intracellular Fe^{3+} ions in live Hep G2 cells with low cytotoxicity [30].

The thiophene-modified rhodamine 6G derivative **23** shows selectivity towards Fe^{3+} and Al^{3+} with the LOD of 5 and 6 μM [31]. The rhodamine-furan-5-carbaldehyde chemosensor **24** shows high Fe^{3+} selectivity with the LOD of 17 nM. The probe **24** is safe for biological use and is non-toxic to living cells [32]. The turn-on colorimetric and fluorescent sensor **25** shows the LOD 0.768 μM Fe^{3+} and bioimage Fe^{3+} ions in live HeLa cells [33]. The probe **26** detects Fe^{3+} , Al^{3+} , and Cr^{3+} with the estimated LOD of 0.29, 0.34, and 0.31 μM , respectively [34]. The probe **26** has been applied to mimic the Boolean logic gates with two and four inputs. The probe **26** has been successfully applied to monitor the selective cations and also the native cellular iron pools. The fluorescence of rhodamine-2-thioxoquinazolin-4-one derivative **27** is increased linearly at 555 nm with the addition of Fe^{3+} from 0 to 75 μM , and the LOD is estimated down to 4.11 μM [35]. The concentration of Fe^{3+} is determined in various real water samples and is successfully applied to monitor intracellular Fe^{3+} ion in living cells. The probe **28** is designed

by reaction rhodamine hydrazide with two equivalents of 2-(thiophen-2-yl)acetyl chloride [36]. The turn-on fluorescence from **28** can be applied to detect Fe^{3+} down to $0.13 \mu\text{M}$, and the probe is suitable in the pH range from 4 to 9. The probe **29** shows a good linearity range from 0.8 to $20 \mu\text{M}$ with the estimated LOD of 11.6 nM [37]. The probe **30**, possessing rhodamine and anthracene, detects Fe^{3+} down to 42 nM and has been applied successfully to monitor Fe^{3+} ions in living cells and zebrafish (Figure 2) [38]. The furfuran-based rhodamine B fluorescent probe **31** can be applied to detect Fe^{3+} down to $0.025 \mu\text{M}$, and the turn-on fluorescence due to the **31**- Fe^{3+} complex formation is shown to be reversed upon addition of $\text{B}_4\text{O}_7^{2-}$ [39].

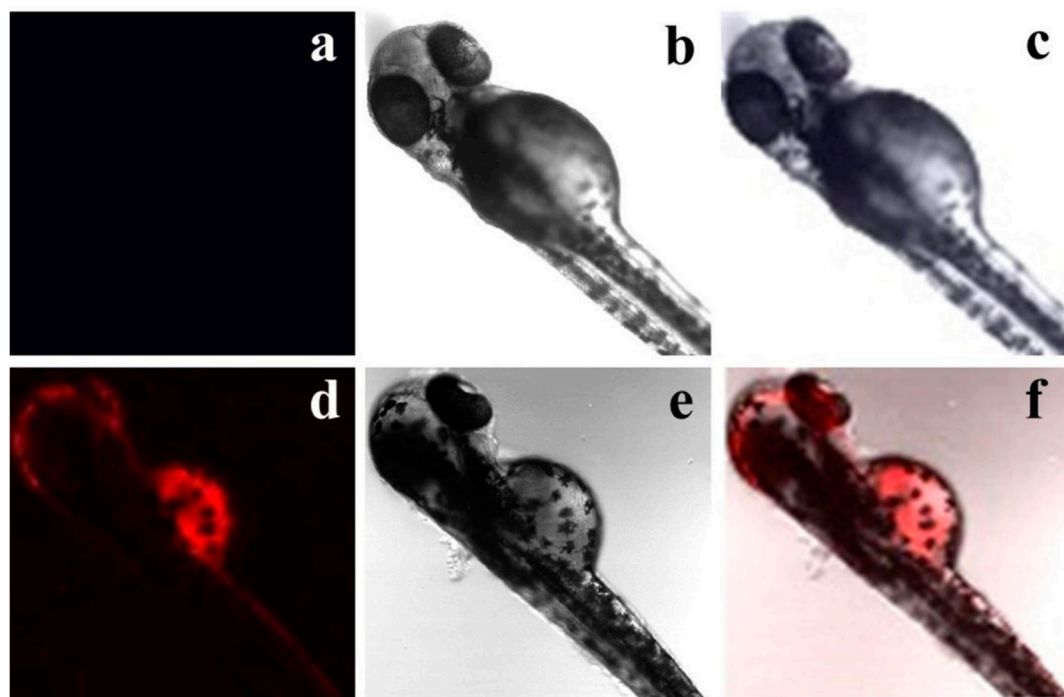


Figure 2. Fluorescence images of Fe^{3+} in zebrafish using the probe **30** ($\lambda_{\text{exc}} = 546 \text{ nm}$, fluorescent signals were collected at $550\text{--}650 \text{ nm}$). (a) Fluorescent image, (b) bright field image, and (c) merged image of zebrafish incubated with the probe **30** (10 mM) for 20 min. (d) Fluorescent image, (e) bright field image, and (f) merged image of probe **30**-loaded zebrafish incubated with Fe^{3+} ($40 \mu\text{M}$) for 20 min (Reproduced from Ref. [38] with permission from Elsevier).

The Fe^{3+} -selective fluorescent turn-on probe **32** is suitable in the pH range from 5 to 9 [40]. The probe **32** has been applied to detect basal level Fe^{3+} and the dynamic changes in Fe^{3+} levels in live bovine aortic endothelial cells (BAEC) at a subcellular resolution that reveal two Fe^{3+} pools in endosomes/lysosomes and mitochondria. The probe **33** forms complex with Fe^{3+} in 2:1 binding ratio and shows significant fluorescence enhancement at 588 nm [41]. The probes detect Fe^{3+} better in the basic condition (pH 7 to 10), and the estimated LOD is 92 nM . The probe **34** fluorescence enhances linearly from 1 to $170 \mu\text{M}$ of Fe^{3+} with the estimated LOD of $1.2 \mu\text{M}$ [42]. The rhodamine-based quinoline conjugated probe **35** shows distinct UV-Vis spectral changes upon addition of Fe^{3+} and Cu^{2+} , but the fluorescence is enhanced selectively in the presence of Fe^{3+} [43]. The turn-on fluorescence from **35** allows to detect Fe^{3+} down to 33 nM , and the probe has been applied to detect Fe^{3+} ions in zebrafish embryos. The furan-2-carbonyl chloride modified rhodamine B derivative **36** selectively forms a complex with Fe^{3+} in 1:1 ratio and shows significant fluorescence enhancement at 582 nm that allows to detect Fe^{3+} down to $0.437 \mu\text{M}$ [44]. The pyridine-type rhodamine B fluorescent probes **37** and **38** are developed to detect Fe^{3+} down to $0.067 \mu\text{M}$ and $0.345 \mu\text{M}$, respectively [45]. Its analytical applicability has been tested by monitoring Fe^{3+} concentrations in various real water samples and live cells. The probe **39**, developed by combining rhodamine and piperonaldehyde, shows LOD of 11.8 nM

Fe³⁺ [46]. The rhodamine-based probe **40** shows high selectivity towards Fe³⁺ (LOD = 0.205 μM) and detects the intracellular Fe³⁺ ions in HeLa cells [47].

The mechanisms like CHEF, PET, excimer formation, C=N isomerization, ESIPT (excited-state intramolecular proton transfer), ICT, etc. are also applied to develop Fe³⁺-selective fluorescent turn-on probes (Table 2). Belfield and his co-workers [48] introduced a novel PET-based reversible fluorescence turn-on probe **41** for the selective detection of Fe³⁺. The probe **41** was designed by connecting boron-dipyrromethene (BODIPY) fluorophore with a 1,10-diaza-18-crown-6-based cryptand that acts as the analyte binding unit. The weakly fluorescent **41** (PET process is active) showed significant fluorescence enhancement at 512 nm ($\lambda_{\text{exc}} = 480$ nm) upon addition of Fe³⁺ in H₂O-CH₃CN (9:1 *v/v*). The fluorescence enhancement occurred due to the inhibition of the PET from cryptand to BODIPY fluorophore upon complexation with Fe³⁺. The probe showed a LOD of 1.3×10^{-7} M and was applied for the detection of intracellular Fe³⁺ ions in living HCT-116 cells. Using the Calix [4] arene framework, the quinoline-appended dipodal fluorescent probe **42** has been developed, and its cations sensing ability has been examined in CH₃CN [49]. Upon complexation of Fe³⁺ with **42** in 1:1 binding ratio, significant fluorescence enhancement has been observed at 418 nm ($\lambda_{\text{exc}} = 310$ nm), and the LOD of 0.334 μM Fe³⁺ has been estimated from the fluorescence titration experiment. Further, the **42**-Fe³⁺ complex has been applied as an intracellular fluorescent agent in MDA-MB-231 cells.

Table 2. Physicochemical properties of some iron(III) selective turn-on probes.

| Probes (L) | Medium | Ex. λ (nm) | Em. λ (nm) | Fe ³⁺ :L | LOD | Ref. |
|------------|---|--------------------|--------------------|---------------------|----------|------|
| 41 | H ₂ O-CH ₃ CN (9:1, <i>v/v</i>) | 480 | 512 | 1:1 | 0.13 μM | [48] |
| 42 | CH ₃ CN | 310 | 418 | 1:1 | 0.334 μM | [49] |
| 43 | Aqueous CH ₃ CN | 314 | 554 | 1:1 | 0.74 nM | [50] |
| 44 | EtOH/0.01 M PBS buffer (<i>v/v</i> , 1:1, pH 7.4) | 465 | 578 | 2:1 | 8 nM | [51] |
| 45 | MeOH-H ₂ O (1:1, <i>v/v</i> , TRIS-HCl buffer, pH = 7.2) | 373 | 398,421,447 | 2:1 | 0.58 μM | [52] |
| 46 | CH ₃ CN:H ₂ O (3:7, <i>v/v</i>) at pH 7 | 376 | 406,429,456 | 2:1 | 0.1 pM | [53] |
| 47 | H ₂ O | 420 | 458 | 1:2 | 1 μM | [54] |
| 48 | CH ₃ CN | 395 | 500 | 1:2 | 0.106 μM | [55] |
| 49 | CH ₃ CN-acetone (<i>v/v</i> = 99:1) | 382 | 501 | 1:1 | - | [56] |
| 50 | CH ₃ CN:H ₂ O (3:7, <i>v/v</i>) | 403 | 524 | - | 0.35 nM | [57] |
| 51 | THF:H ₂ O (6:4, <i>v/v</i>) | 408 | 528 | 1:1 | 0.373 μM | [58] |
| 52 | H ₂ O | 332 | 430 | 1:1 | 0.235 μM | [59] |
| 53 | H ₂ O:EtOH (6:4, <i>v/v</i>) | 397 | 550 | 1:1 | 0.8 ppb | [60] |
| 54 | CH ₃ CN:H ₂ O (1:1, <i>v/v</i>) | 380 | 482 | 1:1 | 0.89 nM | [61] |
| 55 | CH ₃ CN | 380 | 516 | 1:2 | 0.45 μM | [62] |

Nandre et. al. [50] developed a novel fluorescent probe **43** based on the benzo-thiazolo-pyrimidine unit for the selective turn-on sensing of Fe³⁺ in aqueous acetonitrile medium. The probe **43** showed a remarkable fluorescence enhancement at 554 nm ($\lambda_{\text{exc}} = 314$ nm) in the presence of Fe³⁺ due to the inhibition of PET. The sensor formed a host-guest complex in 1:1 stoichiometry with the limit of detection down to 0.74 nM. Further, the sensor was successfully utilized for the qualitative and quantitative intracellular detection of Fe³⁺ in live HepG2 cells and HL-7701 cells by a confocal imaging technique (Figure 3). The diketopyrrolopyrrole-based supramolecular fluorescent probe **44** shows selective response in the presence of Fe³⁺ and Au³⁺ [51]. In EtOH/0.01 M PBS buffer (*v/v*, 1:1, pH 7.4), the weakly emission from **44** shows significant enhancement at 578 nm (465 nm) due to the inhibition of C=N isomerization at the excited state due to the formation of a **44**-Fe³⁺ complex in 1:2 ratio. From the fluorescence enhancement, the LOD for Fe³⁺ has been estimated as 8 nM, and the probe is suitable to detect Fe³⁺ over a pH range from 3 to 8. Besides, the probe **44** is cell-permeable and detects the intracellular Fe³⁺ concentration in human lung adenocarcinoma cells (A549).

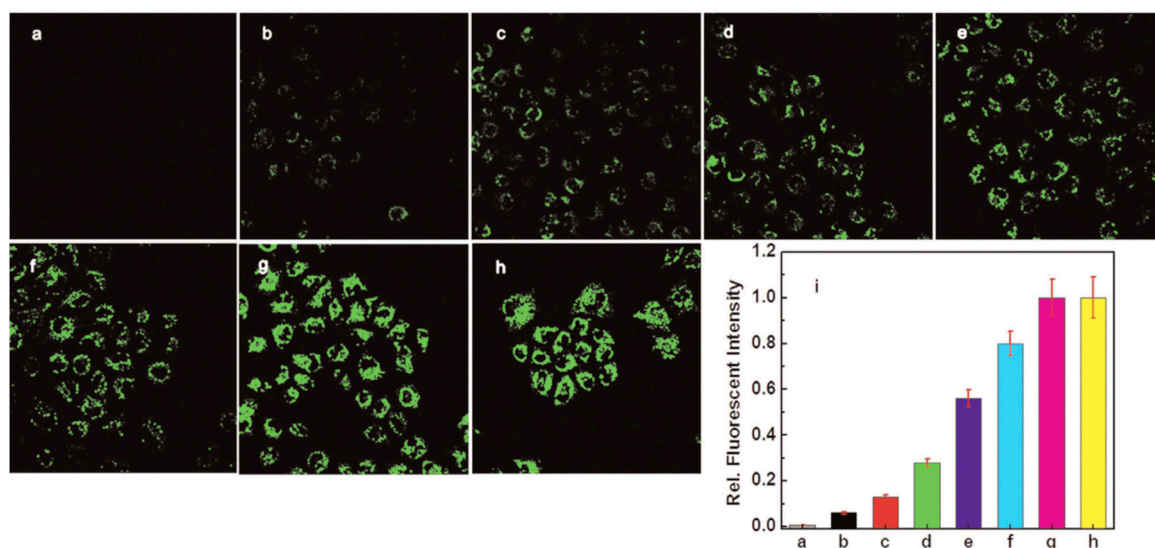
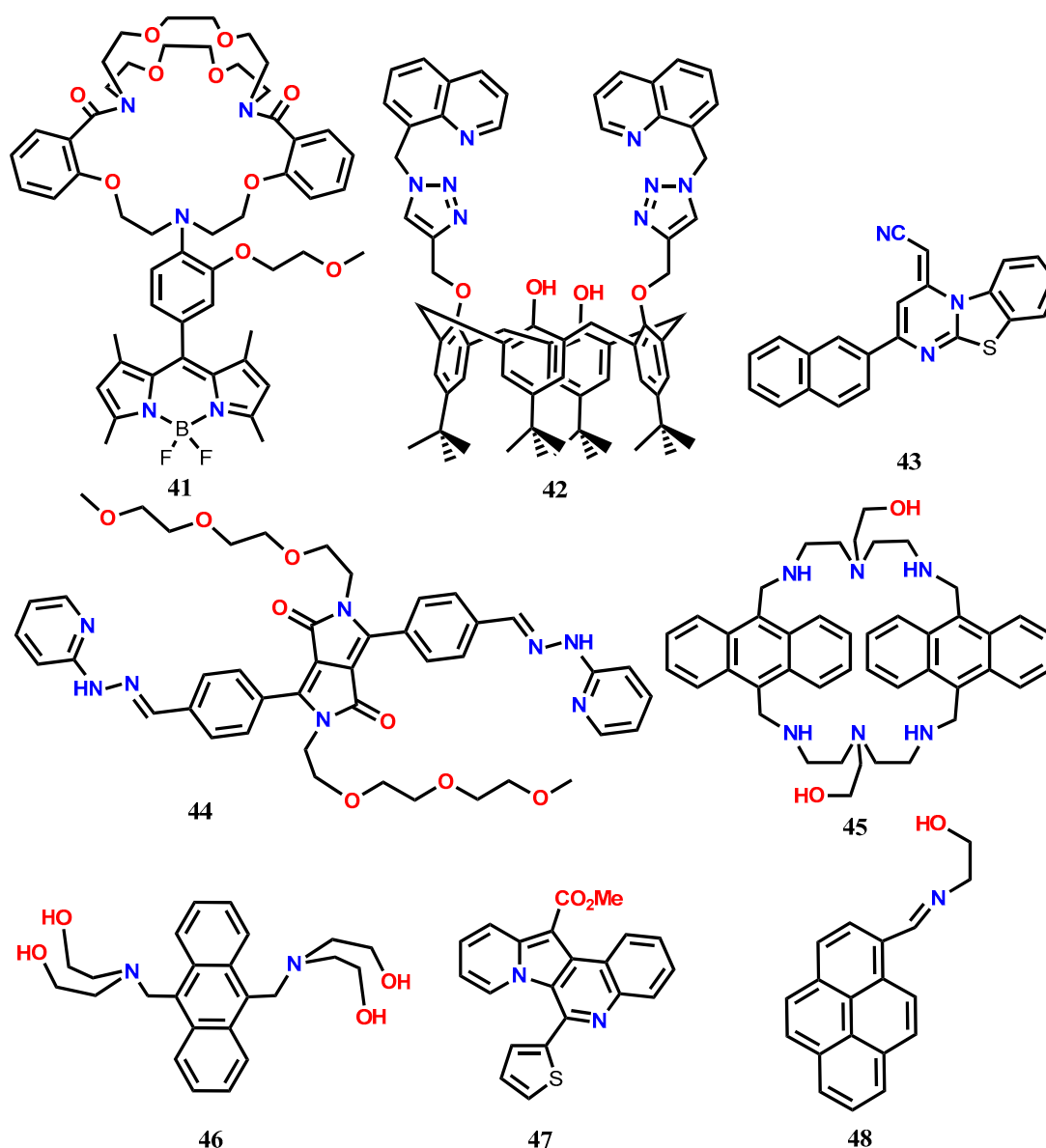


Figure 3. Fluorescence confocal microscopic images of living HL-7701 cells incubated with various concentrations of Fe^{3+} : (a) Cells loaded with 50 μM of iron chelator desferoxamine (DFO) for 40 min. (b) Cells loaded with 10 μM **43** for 10 min as control. (c)–(h) Cells incubated with 0.01, 0.1, 1, 10, 100, and 1000 μM Fe^{3+} , respectively. (i) Quantification of mean fluorescence intensity of the images a–h (scale bar is 20 μm) (Reproduced from Ref. [50] with permission from Elsevier).

The macrocyclic-based fluorescent probe **45** containing anthracene fluorophore shows weak emission at 398, 421, and 447 nm ($\lambda_{\text{exc}} = 373$ nm) in Tris-HCl buffer (20 mM, pH 7.2) containing 50% methanol (*v/v*) [52]. In the presence of Fe^{3+} , the formation of a **45**- Fe^{3+} complex in 1:2 ratio inhibits the PET process, causing significant fluorescence enhancement. Probe **45** shows a linear response range from 1 μM to 10 μM with the LOD of 0.58 μM Fe^{3+} . Confocal imaging discloses that the probe **45** possesses the ability of cell membrane permeability and also the cytosolic Fe^{3+} imaging ability in SKOV-3 cells. Recently, Kim and his co-workers [53] introduced a simple anthracene-based fluorescent turn-on probe **46** substituted with 9,10-diethanolamine for the detection of Fe^{3+} . In $\text{CH}_3\text{CN}:\text{H}_2\text{O}$ (3:7, *v/v*) at pH 7, the weakly emissive probe showed emissions enhancement at 406, 429, and 456 nm characteristic of the anthracene monomer ($\lambda_{\text{exc}} = 376$ nm). Experimental results revealed that the probe **46** formed a complex with Fe^{3+} in 1:2 binding stoichiometry with the association constant of $9.29 \times 10^6 \text{ M}^{-1}$. The chelation-induced enhanced fluorescence (CHEF) effect along with the inhibition of PET resulted in the fluorescence enhancement. The limit of detection of **46** for Fe^{3+} was estimated down to 0.1 pM, and the probe was applied for the monitoring of Fe^{3+} ions in *Candida albicans* (C.A., KCTC-11282) cells. Further, the **46**- Fe^{3+} complex ensemble was applied for the selective detection of CN^- , and also an INHIBIT type logic gate was proposed by taking the two inputs, Fe^{3+} and CN^- .

The novel quinolone-based fluorescent turn-on probe **47** has been developed for the detection of Fe^{3+} and Cr^{3+} [54]. The analytical study of **47** towards Fe^{3+} exhibits a significant fluorescence enhancement at 458 nm ($\lambda_{\text{exc}} = 420$ nm). The formation of a **47**- Fe^{3+} complex in 2:1 ratio restricts the rotation of thiophene, resulting in the fluorescence enhancement both in ethanol and aqueous medium. The probe shows LOD of 1 μM for Fe^{3+} . The probe has been applied for the biological applications in live HepG2 cells to monitor intracellular Fe^{3+} , and also the probe has been applied to detect the autophagosome-lysosome fusion during the autophagy process. The restriction of molecular rotation after forming aggregation also results in significant fluorescent enhancement. The pyrene-based Schiff base **48** solution in CH_3CN undergoes nano-aggregation by adding poor solvent water and shows significant emission enhancement at 465 nm due to the aggregation-induced emission enhancement (AIEE) [55]. The cations sensing ability of **48** in CH_3CN has been tested by adding different metal ions from their water solution, revealing significant fluorescence enhancement at 500 nm ($\lambda_{\text{exc}} = 395$ nm) in the presence of Fe^{3+} , Cr^{3+} , and Al^{3+} . The fluorescence enhancement in the presence of the selective

trivalent metal ions has occurred due to the formation of pyrene excimer upon complexation between **48** and $\text{Fe}^{3+}/\text{Cr}^{3+}/\text{Al}^{3+}$ in 2:1 ratio. With **48**, the LOD is estimated down to 0.106 μM , 0.111 μM , and 0.117 μM for Fe^{3+} , Cr^{3+} , and Al^{3+} , respectively. Besides, the probe shows the ability to detect the selective metal ions within the live Raw264.7 cells. With the excimer formation mechanism, the pyrene-based fluorescent probe **49** has been developed for the selective detection of Fe^{3+} [56]. In acetonitrile-acetone ($v/v = 99:1$), the probe **49** shows weak emission due to the transfer of the electrons on the nitrogen atom to pyrene (PET active). However, upon complexation with Fe^{3+} in 1:1 binding ratio, the probe shows fluorescence enhancement at 507 nm due to the formation of pyrene excimer ($\lambda_{\text{exc}} = 382$ nm). The quantum yield of the probe ($\Phi = 0.001$) is enhanced 41-fold ($\Phi = 0.041$) upon complexation. Besides, the Fe^{3+} -directed formation of a pyrene excimer has also been detected in live HeLa cells.



Han et al. [57] introduced a novel naphthalimide-diethylenetriamine-quinoline-based fluorescent turn-on probe **50** for the selective detection of Fe^{3+} that operated with AIEE and PET mechanisms. The weakly emissive **50** at 513 nm ($\lambda_{\text{exc}} = 403$ nm) in pure CH_3CN showed maximum fluorescence enhancement along with the red-shift from 513 to 524 nm in CH_3CN containing 70% water due to the formation of nano-aggregates, and the red-shift is due to the restriction of intramolecular rotation. The

fluorescent organic nanoparticles (FONs) of **50** showed stable fluorescence in the pH interval from 7–14 and also showed selective fluorescence enhancement in the presence of Fe^{3+} . The FONs showed a linear range from 1 nM to 100 nM with the LOD of 0.35 nM Fe^{3+} . It was proposed that the FONs fluorescence was disrupted due to the PET from the diethylenetriamine unit to the electron-deficient naphthalimide group. Upon complexation of **50** with Fe^{3+} in the FONs, the PET was forbidden, and a dramatic increase in fluorescent intensity was observed. In the cellular medium, the FONs showed low cytotoxicity, and the intracellular Fe^{3+} ions were detected in HeLa by using a fluorescence microscope (Figure 4).

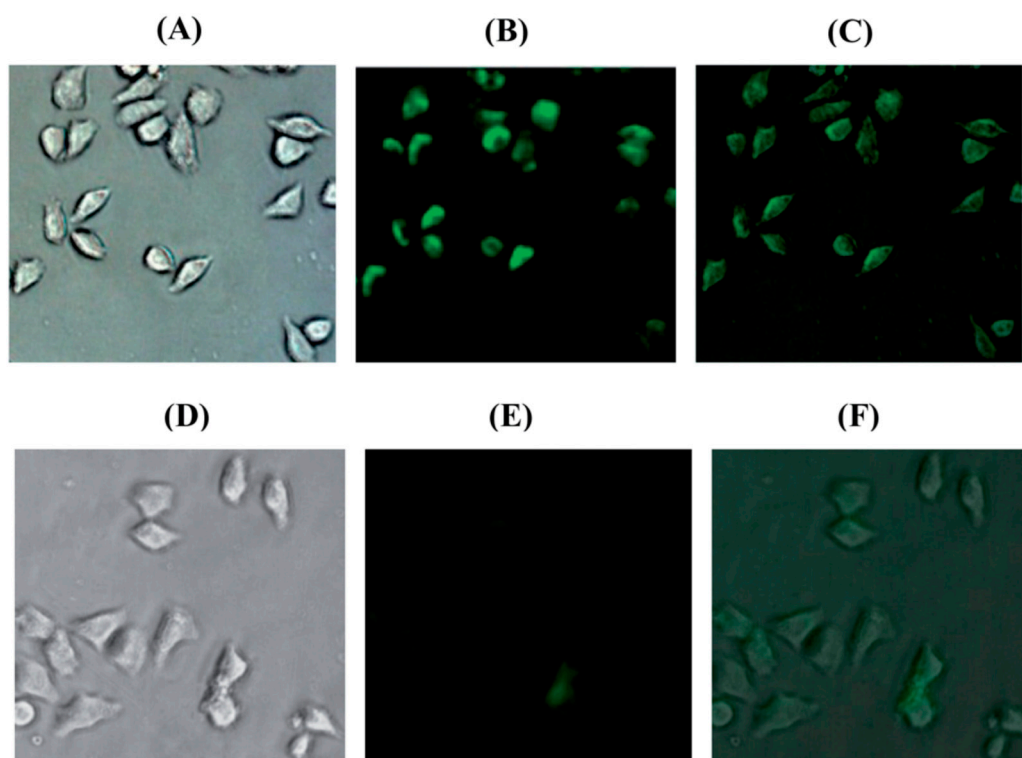


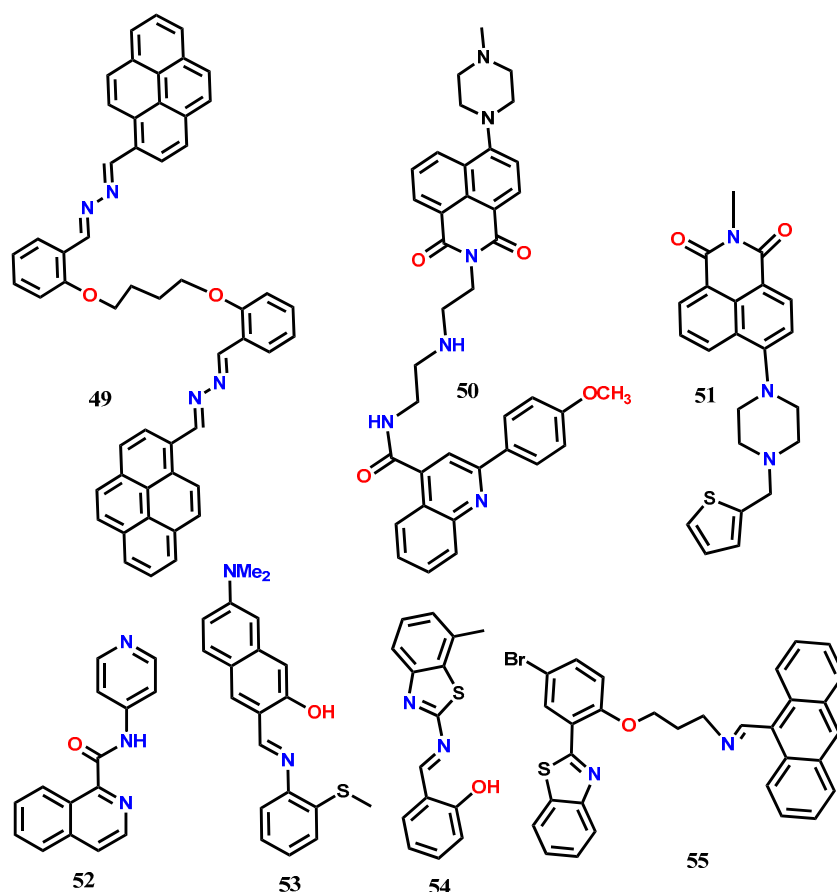
Figure 4. Images of HeLa cells after incubation with FONs (fluorescent organic nanoparticles) **50**. (A) Bright-field image of HeLa cells incubated with Fe^{3+} /FONs (10 nM); (B) fluorescence image of (A); (C) the overlay image of (A) and (B); (D) bright-field image of HeLa cells incubated with FONs (10 nM); (E) fluorescence image of (D); (F) the overlay image of (D) and (E). The fluorescence images were acquired with green light excitation (Reproduced from Ref. [57] with permission from The Royal Society of Chemistry).

Dwivedi et al. [58] utilized the naphthalimide as a signaling unit and the suitably connected thiophene and piperazine rings as recognition unit to develop a highly selective fluorescent turn-on probe **51** to detect Fe^{3+} in solution and live cells. The PET active probe **51** was non-fluorescent in 40% aqueous THF solution, but significant fluorescent was observed at 528 nm ($\lambda_{\text{exc}} = 408$ nm) with the addition of Fe^{3+} . The S atom of thiophene unit and the N atoms of piperazine of **51** formed a complex with Fe^{3+} in 1:1 ratio, inhibiting the PET and resulting in the fluorescence enhancement. With this probe, the LOD was estimated as 0.373 μM , and the probe was applied over a wide pH range (pH 6 to 14) to detect Fe^{3+} . The probe showed excellent biocompatibility and cell permeability to detect the intracellular Fe^{3+} ions in live MCF-7 cells. Further, the in-situ generated Fe^{3+} -**51** complex was applied for the fluorescent turn-off sensing of AcO^- . Applying the PET mechanism, recently, an easy-to-prepare amide-quinoline-based fluorescent probe **52** has been developed for the detection of Fe^{3+} and Al^{3+} in aqueous medium [59]. The probe forms complex with Fe^{3+} and Al^{3+} in the 1:1 binding ratio that diminishes the electron donation from the isoquinoline nitrogen atom towards the pyridyl ring and

inhibits the PET. The suppression of PET at the excited state results in the significant fluorescence enhancement at 430 nm ($\lambda_{\text{exc}} = 332$ nm). The probe shows micromolar LOD of 0.092 and 0.235 μM for Al^{3+} and Fe^{3+} , respectively. Also, the low cytotoxicity of **52** allows monitoring intracellular Fe^{3+} and Al^{3+} ions in live HeLa cells by fluorescence microscopy.

The Schiff-based probe **53** shows fluorescence quenching due to the excited-state intramolecular proton transfer (ESIPT) in $\text{H}_2\text{O}:\text{EtOH}$ (6:4, *v/v*) [60]. With the addition of Fe^{3+} , the formation of a **53-Fe**³⁺ complex in 1:1 ratio suppresses the ESIPT and results in a significant fluorescent enhancement at 550 nm ($\lambda_{\text{exc}} = 397$ nm). The probe shows a wide linear range from 0–200 μM with the LOD of 0.8 ppb. Finally, the probe has been applied to detect intracellular Fe^{3+} ions in the cancer HeLa cells. Another Schiff base probe **54** has been developed for the selective fluorescent turn-on sensing of Fe^{3+} in $\text{CH}_3\text{CN}:\text{H}_2\text{O}$ (1:1, *v/v*) [61]. The probe shows two weak emissions at 430 nm and 574 nm ($\lambda_{\text{exc}} = 380$ nm). The formation of a **54-Fe**³⁺ complex in 1:1 ratio facilitates the charge transfer from the imino group of **54** to Fe^{3+} ion, resulting in an enhanced emission peak centered at 482 nm. The probe can be applied to detect Fe^{3+} down to the nanomolar level (0.89 nM) and is effective at a pH range of 6 to 7. The probe shows good cells permeability, and its ability to detect intracellular Fe^{3+} ions has been tested in live HeLa cells.

Erdemir et. al. [62] introduced an anthracene-based fluorescent probe **55** containing benzothiazole group as a binding unit for the fluorescent turn-on sensing of Fe^{3+} and Cr^{3+} . In CH_3CN , probe **55** shows a weak emission at 428 nm due to the PET process ($\lambda_{\text{exc}} = 380$ nm). Addition of $\text{Fe}^{3+}/\text{Cr}^{3+}$ suppresses the PET, and the complexation of the cations with **55** in 1:2 ratio results in the formation of the anthracenyl static excimer that give distinct fluorescence at 576 nm. The fluorescence titration experiments have estimated the LOD for Cr^{3+} and Fe^{3+} as 0.46 and 0.45 μM , respectively. Finally, the probe has been applied for the fluorescence imaging of living cells and for monitoring Fe^{3+} ions in live PC-3 cells.



3. Ratiometric Fluorescent Probes for Fe(III)

The ratiometric fluorescent probes generally refer to the chemosensors that detect the target analyte from the changes in fluorescence intensity occurring at two emission bands [63]. The ratio of the change in fluorescence intensity of the probe at two different emission peaks is calibrated to monitor the target analyte. Because of the presence of two different emission bands for detection, the ratiometric probes provide several analytical advantages over the probe operated only at a single emission band and also minimize the interferences of the external environments like the concentration of the probe, instrumental parameters, photobleaching, etc. Therefore, great efforts have been given to develop ratiometric fluorescent probes with their potential applications in the field of environmental detection and biological analysis. The well-established mechanisms like fluorescence resonance energy transfer (FRET), through-bond energy transfer (TBET), excimer/excimer formation, intramolecular charge transfer (ICT), etc. can be adopted for the designing of ratiometric fluorescent probes. Several Fe³⁺-selective ratiometric fluorescent probes have been reported in the last few years (Table 3), which are mainly based on the FRET, TBET, and ICT mechanisms.

Table 3. Physicochemical properties of some iron(III) selective ratiometric fluorescent probes.

| Probes (L) | Medium | Ex.λ (nm) | Em.λ (nm) | Fe ³⁺ : L | LOD | Ref. |
|------------|--|-----------|-----------|----------------------|----------|------|
| 56 | Tris HCl-CH ₃ CN (1:1, v/v, pH 7.4) | 420 | 532, 580 | 1:1 | 50 nM | [64] |
| 57 | Tris HCl-CH ₃ CN (1:1, v/v, pH 7.4) | 400 | 532, 583 | 1:1 | 0.03 μM | [65] |
| 58 | EtOH-H ₂ O (2:1, v/v, HEPES buffer, pH 7) | 330 | 455, 585 | 1:1 | 540 nM | [66] |
| 59 | Tris-HCl, Ph = 7.2 | 400 | 442, 538 | 1:1 | 300 nM | [67] |
| 60 | EtOH-H ₂ O (4:1) | 371 | 431, 594 | 1:1 | 6.93 μM | [68] |
| 61 | CH ₃ CN-Tris buffer (9:1, v/v, pH 7.05) | 380 | 515, 605 | 1:1 | 0.64 μM | [69] |
| 62 | EtOH | 420 | 520, 577 | 1:1 | 0.418 μM | [70] |
| 63 | CH ₃ OH/H ₂ O (2/3, v/v, pH = 7.2) | 370 | 470, 558 | 1:1 | 53.9 nM | [71] |
| 64 | EtOH-H ₂ O (9:1, v/v, Tris-HCl, pH = 7.4) | 450 | 475, 550 | 1:1 | 4.05 μM | [72] |
| 65 | CH ₃ OH-H ₂ O (4:6, v/v) | 420 | 535, 585 | 1:1 | 0.105 μM | [73] |
| 66 | CH ₃ CN-HEPES buffer (1/4, v/v, pH 7.4) | 365 | 412, 445 | 1:1 | 3.5 μM | [74] |
| 67 | CHCl ₃ -MeOH (1:1, v/v) | 300 | 400, 480 | 1:1 | 1.17 μM | [75] |
| 68 | DMSO/H ₂ O (1:99, v/v v/v) | 320 | 443, 380 | 1:1 | 2 μM | [76] |
| 69 | CH ₃ CN/Tris buffer = 9:1, v/v, pH = 7.4 | 380 | 431, 517 | 1:2 | 4.47 μM | [77] |
| 70 | Aqueous CH ₃ CN | 420 | 504, 526 | 1:1 | 10 nM | [78] |

The FRET-based probe consists of two fluorophore units separated by a spacer, where the excited state of one fluorophore (donor) transfers its energy to the closely located another fluorophore (acceptor) in a non-radiative manner, and then the energy is released in a radiative manner from the second fluorophore [63]. In designing FRET-based probes, care must be taken that the donor to acceptor distance and orientation is appropriate for energy transfer. Besides, there must be spectral overlap between the fluorescence profile of the donor fluorophore with the UV-Vis absorption spectra of acceptor fluorophore. By utilizing the naphthalimide and rhodamine dyes, the FRET-based fluorescent probe **56** has been designed for the ratiometric detection of Fe³⁺ in aqueous acetonitrile (1:1, v/v, 0.01 M Tris HCl-CH₃CN, pH 7.4) medium [64]. In this probe, the triazole appended quinoline-rhodamine conjugate acts as a selective ionophore for Fe³⁺ and FRET energy acceptor, whereas the 8-piperazinonaphthalimide moiety acts as the FRET energy donor. In the presence of Fe³⁺, the emission at 532 nm from the naphthalimide moiety is decreased, and a new emission band appears at 580 nm ($\lambda_{exc} = 420$ nm). The ratiometric response from the probe **56** is due to the complexation-induced opening of the spirocyclic ring of the rhodamine moiety that facilitates the FRET from the naphthalimide donor. The FRET is possible because of the excellent spectral overlap of the naphthalimide emission spectrum with the absorption spectrum of the rhodamine unit of **56**. With this probe, the LOD has been estimated down to 5×10^{-8} M (~3 ppb) and applied successfully for the monitoring of trace levels of intracellular Fe³⁺ ions in NIH 3T3 cells (Figure 5). Subsequently, the same group uses the naphthalimide-rhodamine combination to develop a FRET-based multi-analytes (Fe³⁺, Al³⁺, and Cr³⁺)-selective fluorescent probe **57** [65]. This probe shows a decrease in the naphthalimide emission at 532 nm and concomitant appearance of a new emission peak at 583 nm upon addition of Fe³⁺, Al³⁺, and Cr³⁺ ions in aqueous acetonitrile (1:1, v/v, 0.01 M Tris HCl-CH₃CN, pH 7.4) medium. The formation of the metal complex

between **57** and the metal ions in 1:1 binding stoichiometry opens the spirocyclic ring of the rhodamine unit, allowing the FRET process to give the ratiometric signal. Also, the probe has been applied to detect the intracellular Fe^{3+} ions in W138 cells.

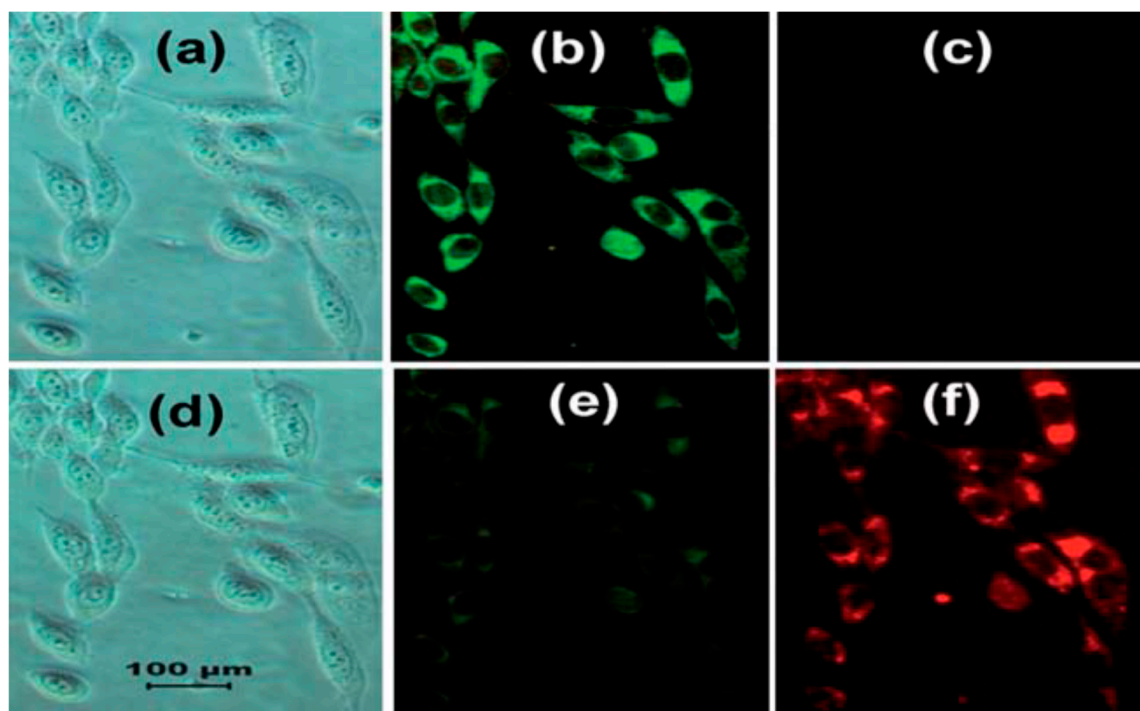


Figure 5. Bright-field and fluorescence microscopic images of NIH 3T3 cells obtained using a Leica DM IRB microscope equipped with an EBQ-100 UV-lamp. Top row: NIH 3T3 cells incubated with **56** (5 mM) for 30 min and observed under bright-field (**a**), green channel (**b**), and red channel (**c**). Bottom row: NIH 3T3 cells incubated with **56** (5 mM) for 30 min, treated with Fe^{3+} (5 mM) for 15 min, and observed under bright-field (**d**), green channel (**e**), and red channel (**f**) (Reproduced from Ref. [64] with permission from The Royal Society of Chemistry).

Das and his co-workers [66] developed the FRET-based fluorescent probe **58** containing a 2-hydroxynaphthalene unit as a donor and rhodamine B as an acceptor for the selective detection of Cr^{3+} and Fe^{3+} in HEPES buffered (0.1 M) EtOH- H_2O (2:1, *v/v*, pH 7). The fluorescence of **58** at 455 nm ($\lambda_{\text{exc}} = 330$ nm, blue fluorescence) from the 2-hydroxynaphthalene moiety is quenched, and a new fluorescence band appears at 585 nm (red fluorescence) in the presence of Fe^{3+} and Cr^{3+} . The complexation-induced ring-opening of the spirolactam unit has resulted in energy transfer from the donor to the acceptor unit. With **58**, the concentration of Cr^{3+} and Fe^{3+} can be detected down to 10 nM and 0.54 μM , respectively. Further, the probe has been applied for the detection of intracellular Cr^{3+} and Fe^{3+} ions in *Bacillus sp.* cells and *Candida albicans* cells by recording the fluorescence images. Applying the FRET mechanism, the rhodamine spirolactam has been connected to the blue fluorescent water-soluble ionic conjugated polymers (CPs) to develop a ratiometric probe for Fe^{3+} [67]. Exciting the probe **59** at 400 nm in a buffer solution (Tris-HCl, pH = 7.2), the fluorescence of CPs at 442 nm is quenched, and a new peak appears at 538 nm in the presence of Fe^{3+} due to the complexation-induced spirocyclic ring-opening of rhodamine 6G. Also, the quenching of CPs emission is due to the possible FRET to the rhodamine 6G unit. Using the ratiometric signal changes (I_{538}/I_{442}), the detection limit has been estimated as 0.3 μM . The FRET efficiency between CPs and rhodamine 6G is 61.8%, and the distance between the acceptor and donor as 4.06 nm, supporting the efficient FRET between the two fluorophores. Using the probe **59**, the confocal fluorescence imaging experiment has been carried to monitor the intracellular Fe^{3+} ions in live HeLa cells.

Chen et al. [68] introduced a new ratiometric fluorescent sensor **60** by suitably combining the naphthalene and rhodamine dyes for the selective detection of mitochondrial Fe^{3+} in live HeLa cells. The fluorescence of **60** at 431 nm was quenched, and concomitantly a new emission appeared at 594 nm ($\lambda_{\text{exc}} = 371$) upon addition of Fe^{3+} in EtOH- H_2O (4:1). The ratiometric emission from the probe **60** was observed due to the possible FRET from the conjugated naphthalene donor to the rhodamine acceptor. Without any noticeable interference from other tested metal ions, the concentration of Fe^{3+} could be detected down to 6.93 μM . Besides, due to the presence of a lipophilic alkyltriphenylphosphonium (alkylITPP) cation that helps in passing directly through the phospholipid bilayers and accumulate selectively within the mitochondria inside cells, the probe **60** showed satisfactory cell permeability and detected the mitochondrial Fe^{3+} in live HeLa cells (Figure 6).

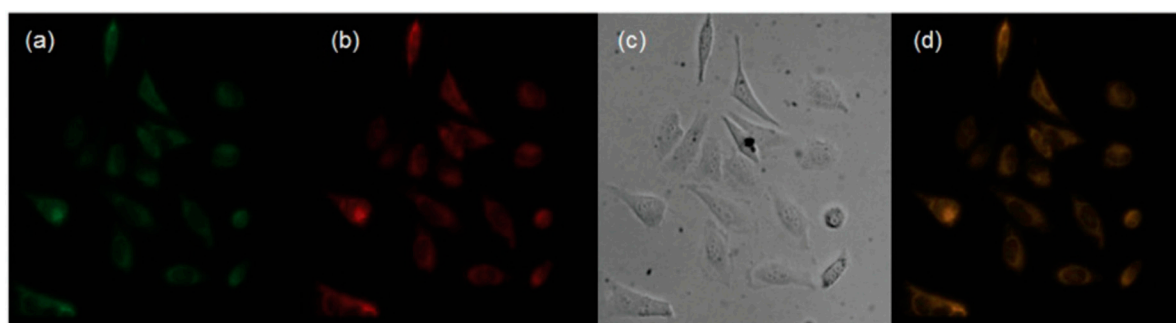
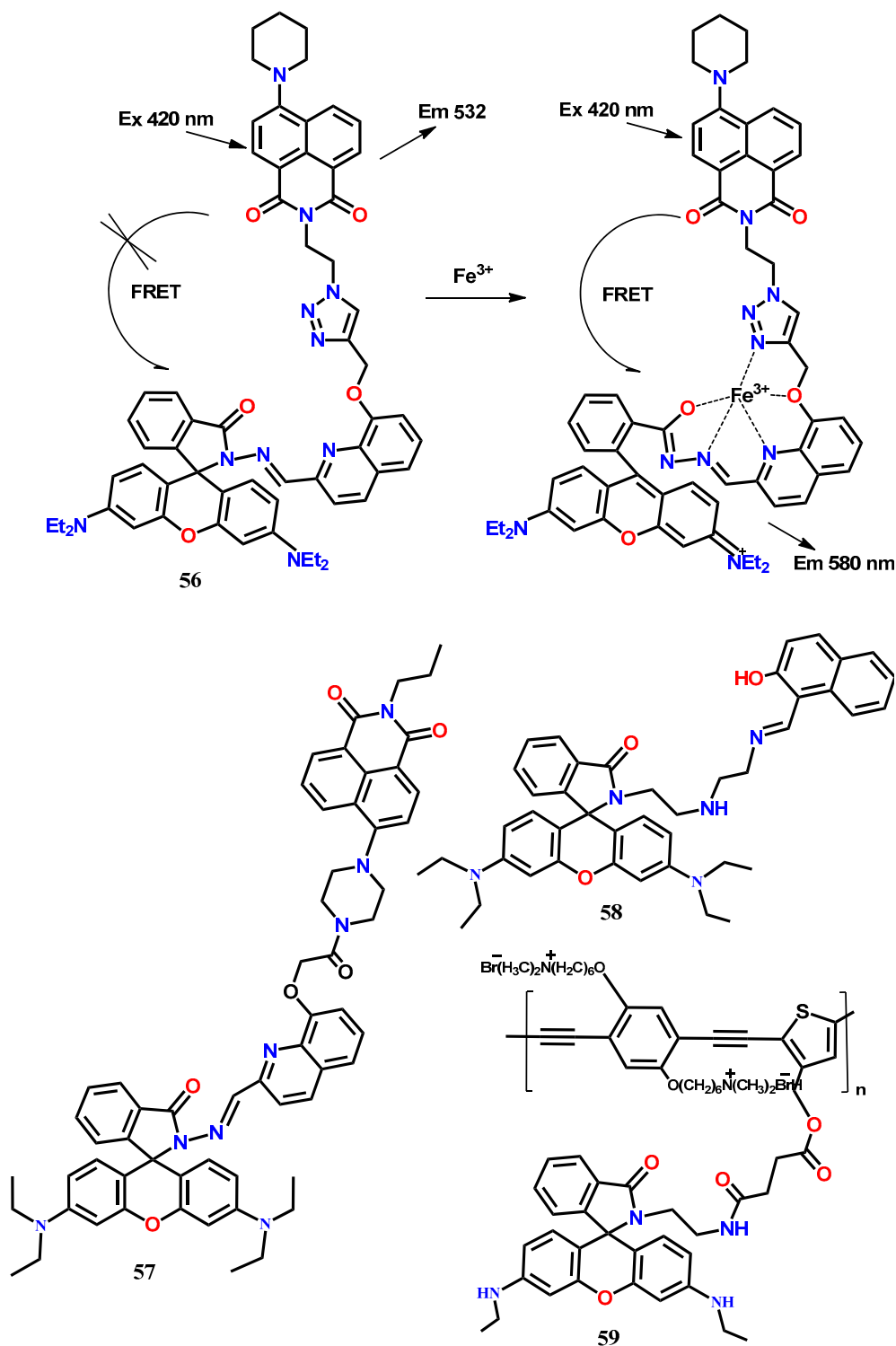


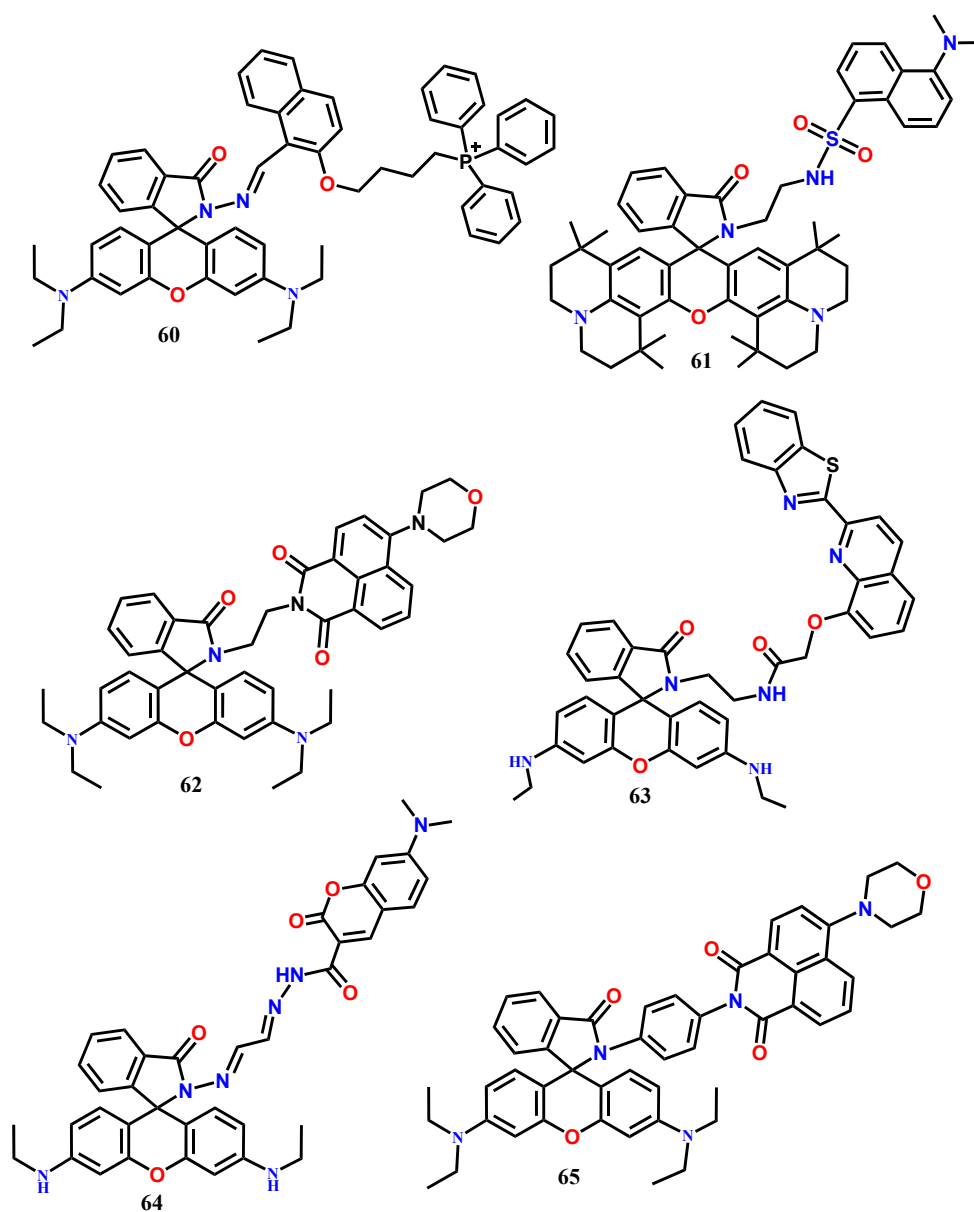
Figure 6. Localization of **60** in mitochondria of HeLa cells. **60** (5 μM) and MitoTracker Green FM (200 nM) were loaded into HeLa cells: (a) fluorescence image of MitoTracker Green FM (excitation: 488 nm, emission: 450–550 nm); (b) fluorescence image of **60** with Fe^{3+} (excitation: 515 nm, emission: 550–650 nm); (c) bright-field of HeLa cells; (d) merged image (Reproduced from Ref. [68] with permission from The Royal Society of Chemistry).

The FRET-based fluorescent probe **61** containing a dansyl unit as a donor and rhodamine 101 as an acceptor has been developed to detect Fe^{3+} in CH_3CN -Tris buffer (9:1, *v/v*, pH 7.05) [69]. Fe^{3+} -induced ring-opening of the spirolactam rhodamine moiety results in the formation of fluorescent derivative that can serve as the FRET acceptor ($\lambda_{\text{exc}} = 380$ nm). Ratiometric sensing of Fe^{3+} is accomplished by plotting the fluorescence intensity ratio at 605 nm and 515 nm versus Fe^{3+} ions concentration. The large Stokes shift (225 nm) shown by the probe can eliminate the back-scattering effects of excitation light. The probe displays a linear response to Fe^{3+} in the range of 5.5–25 μM with a detection limit of 0.64 μM . Combining naphthalimide and rhodamine B by using the ethylenediamine connector, a new Fe^{3+} -selective FRET-based ratiometric fluorescent probe **62** has been developed [70], where the naphthalimide acts as an energy donor, while the spirocyclic ring-open form of rhodamine as the energy acceptor. Upon complexation with Fe^{3+} , the emission from the naphthalimide unit of the probe **62** at 520 nm is decreased, and a significant enhancement of the characteristic fluorescence of the rhodamine is observed at 577 nm ($\lambda_{\text{exc}} = 420$ nm) in ethanol solution. The probe shows a linear range for Fe^{3+} from 0.2 to 1 μM with the LOD of 0.418 μM . Besides, the probe shows the cell permeability to detect the intracellular Fe^{3+} ions in live EC109 cells in the fluorescence imaging study.

The FRET-based benzothiazole conjugated quinoline derivative appended with rhodamine-6G ratiometric fluorescent probe **63** has been introduced for the detection of Fe^{3+} [71]. The probe shows a strong emission at 470 nm ($\lambda_{\text{exc}} = 370$ nm) from the benzothiazole moiety in $\text{CH}_3\text{OH}/\text{H}_2\text{O}$ (2/3, *v/v*, pH = 7.2). The complexation-induced opening of the spirocyclic ring of the rhodamine unit results in FRET from the energy donor (benzothiazole moiety) to the energy acceptor (rhodamine-6G domain). As a result, a new peak appears at 558 nm with the gradual decrease in the intensity at 470 nm. The ratio of the emission intensities at the two wavelengths (I_{558}/I_{470}) exhibits good linearity with the added concentration of Fe^{3+} from 0–14 μM with the estimated LOD of 53.9 nM. The FRET-based probe **64** has been designed by suitably connecting the coumarin (energy donor) with the rhodamine moiety (energy

acceptor) [72]. In EtOH-H₂O (9:1, *v/v*, Tris-HCl, pH = 7.4), the receptor shows only the coumarin emission band at 475 nm ($\lambda_{\text{exc}} = 450$ nm), whereas a new emission band appears at 550 nm upon addition of Fe³⁺ due to the complexation-induced opening of the spirocyclic ring of the rhodamine. With this probe, the concentration of Fe³⁺ can be detected down to 4.05 μM .





The FRET-based energy transfer mechanism is most popular for the designing of ratiometric fluorescent probes, and their FRET efficiency is primarily controlled by the spectral overlap between the emission spectrum of the energy donor and the absorption spectrum of the energy acceptor. In contrast to the FRET systems, the through-bond energy transfer (TBET) systems are not limited to such spectral overlap for the energy transfer between two fluorophores. The probes based on TBET mechanisms are well-known to show fast energy transfer rates and large pseudo-Stokes shift. In probe **65**, the energy donor (4-morpholine)-1,8-naphthalimide moiety is linked to the energy acceptor rhodamine by a rigid and conjugated spacer *p*-phenylenediamine [73]. This rigid connection efficiently prevents the fluorescence quenching of naphthalimide. In the absence of Fe^{3+} , the excited energy of the naphthalimide donor is not transferred to the closed form of rhodamine acceptor, and the characteristic peak of naphthalimide is observed at 535 nm in $\text{CH}_3\text{OH-H}_2\text{O}$ (4:6, *v/v*). The complexation of **65** with Fe^{3+} opens the spirocyclic ring of the rhodamine ring, resulting in a significant fluorescence enhancement at 585 nm ($\lambda_{\text{exc}} = 420$ nm). Simultaneously, the naphthalimide emission at 535 nm quenches due to the TBET. The ratiometric probe **65** shows a linear fluorescence response from 0 to 20 μM with the LOD of 0.105 μM Fe^{3+} . Further, the probe has been applied for ratiometric fluorescence imaging of Fe^{3+} ions in living EC109 cells (Figure 7).

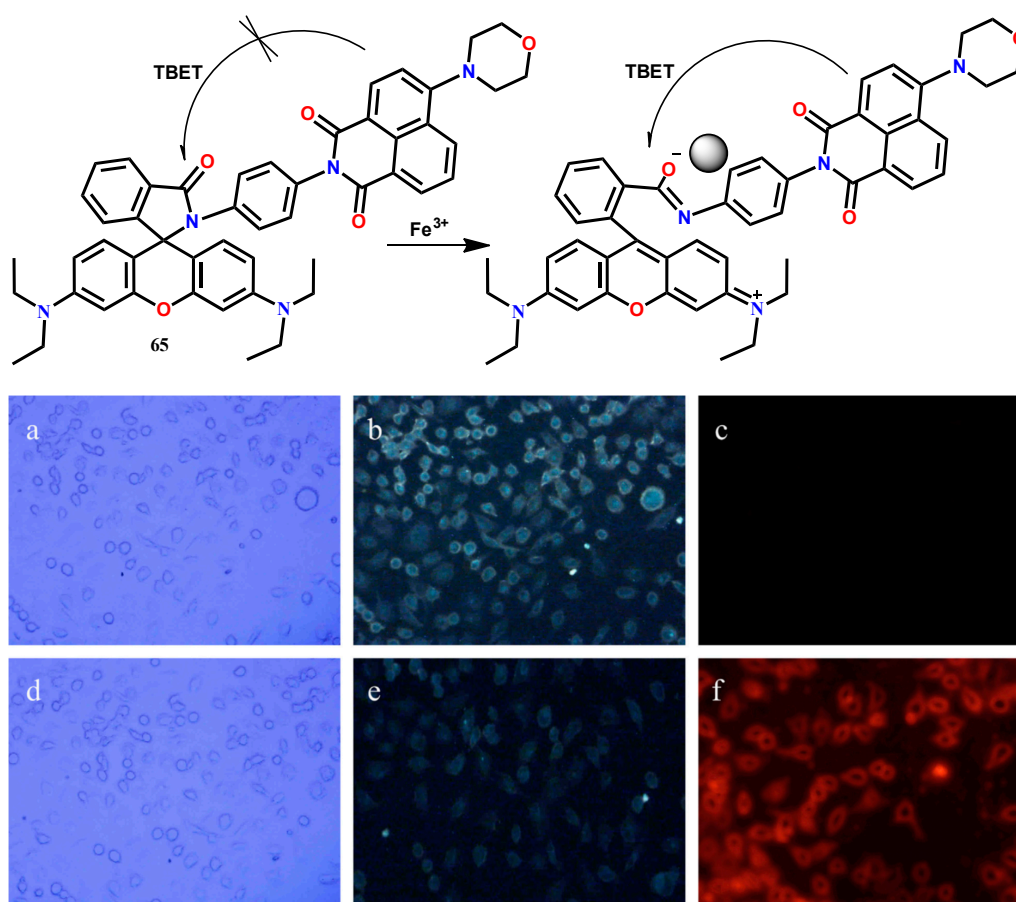
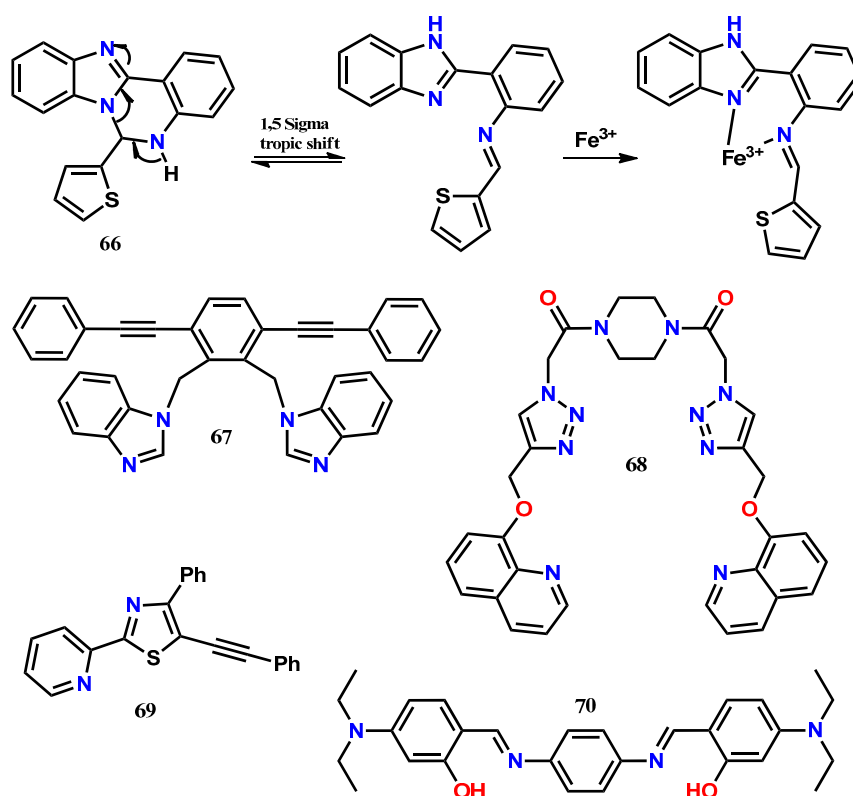


Figure 7. Images of EC109 cells treated with the ratiometric **65**: (a) bright-field image of EC109 cell incubated with **65** (5 μM); (b) fluorescence image from green channel; (c) fluorescence image from red channel; (d) bright-field image of EC109 cell incubated with **65** (5 μM) for 15 min, and then further incubation with Fe^{3+} (5 μM) for 15 min at 37 $^{\circ}\text{C}$; (e) fluorescence image from green channel; (f) fluorescence image from red channel (Reproduced from Ref. [73] with permission from Elsevier).

Chattopadhyay and his co-workers [74] introduced the ratiometric fluorescent probe **66**, which undergoes a 1,5-sigmatropic shift in solution to form the benzimidazole derivative with the more chelating environment. The intensity of the weakly fluorescence benzimidazole derivative of **66** at 412 nm ($\lambda_{\text{exc}} = 365$ nm) was decreased, and a new fluorescence peak appeared at 445 nm upon addition of Fe^{3+} in CH_3CN -HEPES buffer (1/4, *v/v*, pH 7.4) due to the chelation enhanced fluorescence (CHEF) effect. Similar ratiometric fluorescence changes were also observed in the presence of Fe^{2+} . With **66**, the ratiometric fluorescence response could be used to detect Fe^{3+} and Fe^{2+} ions down to 3.5 μM and 2 μM , respectively. Further, the probe was applied to detect intracellular Fe^{3+} ions in live HeLa cells. Based on the efficient ligand metal charge-transfer effect, the piperazine-based dipodal fluorescent probe **67** appended with 8-hydroxyquinoline has been introduced for the ratiometric detection of Fe^{3+} [75]. In CHCl_3 -MeOH (1:1, *v/v*), the probe has shown monomer emission of the quinoline moiety at 400 nm ($\lambda_{\text{exc}} = 300$ nm). Upon addition of Fe^{3+} , the emission peak at 400 nm is quenched, and a new broad emission appears at 480 nm. This ratiometric fluorescence quenching in the presence of Fe^{3+} is attributed to the strong interaction of Fe^{3+} with the triazolmethoxyquinoline (as tridentate ligand) motifs of **67**. Calibrating the intensity ratio (I_{480}/I_{400}) with the change in concentration of Fe^{3+} gives LOD of 1.17 μM . Receptor **67** is cells permeable and detect intracellular Fe^{3+} ions in live HeLa cells with no cytotoxicity. Sequentially, the **67**- Fe^{3+} complex ensemble is applied for the selective detection of fluoride anion.

The dipodal clip-type ratiometric fluorescent probe **68** containing two benzimidazole groups has been applied for the selective detection of Cr^{3+} and Fe^{3+} ions in DMSO/ H_2O (1:99, v/v) [76]. When excited at 320 nm, the probe **68** fluorescence at 443 nm quenches and simultaneously enhances at 378/380 nm upon addition of $\text{Cr}^{3+}/\text{Fe}^{3+}$. It has been proposed that the blue-shift in the fluorescence of **68** is due to the intramolecular charge transfer (ICT), whereas the enhancement of fluorescence intensity upon $\text{Cr}^{3+}/\text{Fe}^{3+}$ complexation is most likely due to the inhibition of PET processes. With the probe, the minimum detection limit is estimated as 25 μM and 2 μM for Cr^{3+} and Fe^{3+} , respectively. Further, the selective UV-Vis spectral changes of **68** in the presence of Fe^{3+} allow discriminating the presence of both Cr^{3+} and Fe^{3+} . Using the robust fluorophore 2-pyridylthiazole and ICT mechanism, an easy-to-prepare ratiometric fluorescence probe **69** has been developed for the selective detection of Fe^{3+} [77]. In an aqueous system ($\text{CH}_3\text{CN}/\text{Tris}$ buffer = 9:1, v/v , pH = 7.4), the probe emission at 431 nm quenches with the concomitant appearance of a new emission at 517 nm ($\lambda_{\text{exc}} = 380$ nm) in the presence of Fe^{3+} . The LOD of this probe is estimated to be 4.47 μM for Fe^{3+} . Recently, the easy-to-prepare linear Schiff base receptor **70** has been developed for the ratiometric detection of Fe^{3+} and fluorescence turn-off sensing of Cu^{2+} in aqueous acetonitrile medium [78]. Upon addition of Fe^{3+} , receptor **70** induces a selective fluorescence enhancement with a 22 nm red-shift from 504 nm to 526 nm, making it easily distinguishable from the other tested metal ions. The fluorescence enhancement is observed presumably due to deprotonation of the phenolic-OH protons on coordination with Fe^{3+} , inhibiting the $-\text{C}=\text{N}$ isomerization and/or the ESIPT process in the excited state. Also, the red-shift indicates that the possible ICT occurs in **70** on interaction with Fe^{3+} . In contrast, the fluorescence of **70** quenches upon addition of Cu^{2+} . The quenching by Cu^{2+} is most likely due to an energy transfer process occurring between **70** and paramagnetic Cu^{2+} . From the emission titrations, the LOD for the sensing of Fe^{3+} and Cu^{2+} ions are estimated to be 10 nM and 15 nM, respectively. Besides, the organic nanoparticles (ONPs) of the probe **70** has been developed and applied for the detection of Fe^{3+} and Cu^{2+} in different drug supplements available in the market. Also, the probe fluorescence response has been applied to mimic the IMP (IMPLICATION) type logic gate with the two-inputs as Fe^{3+} and Cu^{2+} .



4. Fluorescent Chemodosimeters for Fe(III)

The design of Fe³⁺-selective fluorescent turn-on probes with high selectivity and sensitivity can be achieved by chemodosimeter approach, where the Fe³⁺ ions mediate the breaking of some important bonds in the probe, leading to the irreversible transduction of a detectable fluorescent signal [79]. Recently, a few one-time use fluorescent chemodosimeters are reported for the detection of Fe³⁺ (Table 4) and are also applied successfully to detect the intracellular Fe³⁺ ions in live cells by bioimaging.

Table 4. Physicochemical properties of some iron(III) selective reaction-based fluorescent probes.

| Probes (L) | Medium | Ex. λ (nm) | Em. λ (nm) | LOD | Ref. |
|------------|---|--------------------|--------------------|---------------|------|
| 71 | HEPES aqueous buffer (pH 7, 40 mM) | 585 | 615 | - | [80] |
| 72 | Potassium phosphate buffer/acetone (1:4, v/v, pH = 7) | 360 | 522 | 0.12 μ M | [81] |
| 73 | Aqueous DMSO | 325 | 441 | 4.3 μ M | [82] |
| 74 | DMSO/H ₂ O (v/v = 70:30) | 396 | 440 | 1.37 μ M | [83] |
| 75 | DMSO/H ₂ O (v/v = 9/1, HEPES buffer, pH = 7.4) | 390 | 440 | 75.7 nM | [84] |
| 76 | MeOH/H ₂ O (9/1, v/v) | 388 | 430 | 0.118 μ M | [85] |
| 77 | THF-H ₂ O (8:2) | 330 | 430 | 0.38 nM | [86] |

Chen et. al. [80] introduced a novel chemodosimeter-based fluorescent probe **71**, consisted of a BODIPY dye, as a signal transducer that is suitably linked to a hydroxylamine unit (Figure 8). Above pH = 5.8, the electron-donating ability from the hydroxylamine to the fluorophore unit quenched the fluorescence at 615 nm ($\lambda_{exc} = 585$ nm) due to the PET. In HEPES aqueous buffer (pH 7, 40 mM), the addition of Fe³⁺ selectively oxidized the hydroxylamine that inhibited the PET process, and a significant fluorescence enhancement was observed (from $\Phi = 0.01$ to $\Phi = 0.35$). The probe **71** showed a good linear dependence of fluorescence intensity on Fe³⁺ concentration (0–50 μ M) and applied successfully for the monitoring of Fe³⁺ concentration in live MCF-7 cells by using the confocal fluorescence microscope (Figure 8).

Subsequently, considering the ability of Fe³⁺ to mediate the deprotection of acetal reaction, the ratiometric fluorescent probe **72** has been designed for the highly selective detection of Fe³⁺ in 20 mM potassium phosphate buffer/acetone (pH 7, 1:4 (v/v)) at room temperature [81]. The acetal group of **72** is deprotected into aldehyde by Fe³⁺, increasing the π -electrons conjugation, and, therefore, the effective ICT from the phenanthroline unit to the aldehyde results in the red-shift in the emission band from 390 nm to 522 nm ($\lambda_{exc} = 360$ nm). The fluorescence titration of **72** with Fe³⁺ shows satisfactory linearity in the range of 0–30 μ M between the emission ratio (I_{522}/I_{390}) and the concentration of Fe³⁺. With **72**, the concentration of Fe³⁺ can be detected down to 0.12 μ M. Further, the probe has been successfully applied for imaging Fe³⁺ in living pancreatic cancer cells (Figure 9).

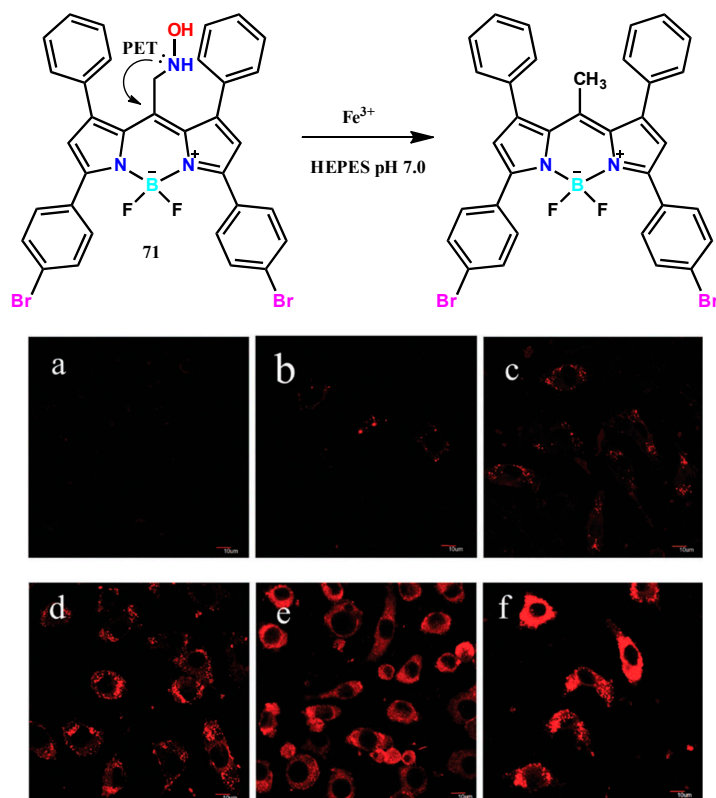


Figure 8. Confocal fluorescence images of living MCF-7 cells incubated with various concentrations of Fe^{3+} . MCF-7 cells loaded with **71** and Fe^{3+} for 15 min of (a) Control, (b) 0.01 mM, (c) 0.1 mM, (d) 1 mM, (e) 10 mM, and (f) 100 mM. Scale bar is 10 μm (Reproduced from Ref. [80] with permission from The Royal Society of Chemistry).

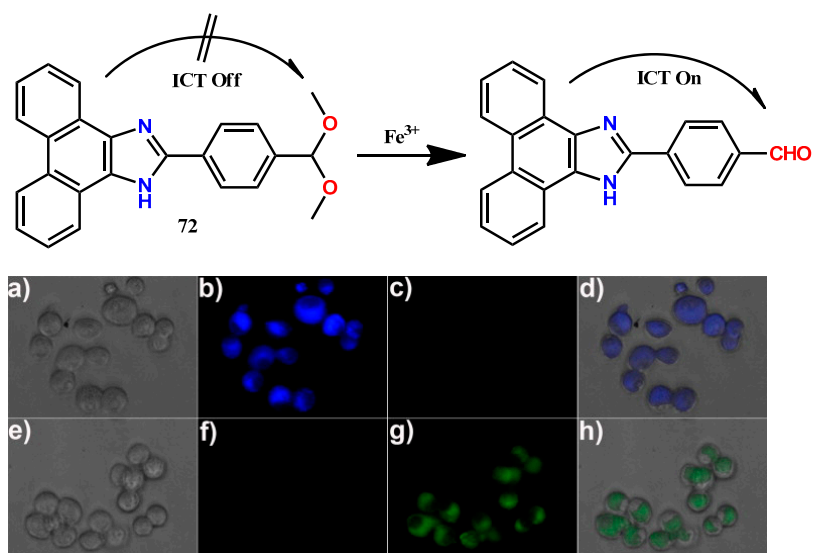
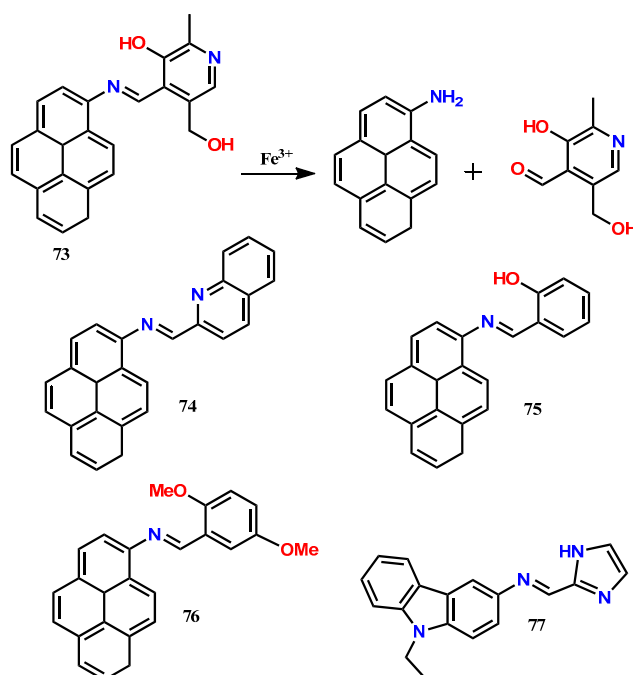


Figure 9. The design concept of fluorescent ratiometric probe **72** for Fe^{3+} . Fluorescence and bright-field images of pancreatic cancer cells. (a) Brightfield image of the cells stained with probe **72** (1 μM) for 30 min; (b) fluorescence image of (a) with emission at 445 ± 10 nm; (c) fluorescence image of (a) with emission at 530 ± 10 nm; (d) an overlay image of (a–c); (e) bright-field image of cells pretreated with Fe^{3+} (50 μM) for 30 min and then further incubated with probe **72** (1 μM) for 30 min; (f) fluorescence image of (e) with emission at 445 ± 10 nm; (g) fluorescence image of (e) with emission at 530 ± 10 nm; (h) an overlay image of (e–g) (Reproduced from Ref. [81] with permission from Elsevier).

Sahoo and his co-workers [82] introduced an easy-to-prepare chemodosimeter-type optical chemosensor **73** for the selective detection of Fe^{3+} by condensing 1-aminopyrene with pyridoxal. Probe **73** showed weak emission at 441 nm ($\lambda_{\text{exc}} = 325$ nm) due to the PET process occurring from the pyridoxal imine to the pyrene fluorophore. Addition of Fe^{3+} hydrolyzed the imine linkage of **73**, leading to the back-formation of 1-aminopyrene and pyridoxal, resulting in a significant fluorescence enhancement at 441 nm in the aqueous DMSO medium. The probe **73** showed good linearity from 0 M to 6.98×10^{-5} M with the limit of detection down to 4.3 μM for Fe^{3+} . The probe **73** was highly specific for the detection of Fe^{3+} , and the concentration of Fe^{3+} could be monitored by using both spectrophotometer and smartphone. Besides, the probe **73** could be applied to monitor Fe^{3+} within the live HeLa cells. With a similar approach, three more Fe^{3+} -selective fluorescent probes **74–76** have been reported [83–85]. The probe **74** shows significant fluorescence enhancement at 440 nm ($\lambda_{\text{exc}} = 396$ nm) selectively in the presence of Fe^{3+} in DMSO/ H_2O ($v/v = 70:30$) due to the Fe^{3+} -mediated hydrolytic cleavage of the imine linkage [83]. Using **74**, the concentration of Fe^{3+} can be detected down to 1.37 μM and successfully applied to detect intracellular Fe^{3+} ions in live RAW264.7 cells by imaging experiment. The same group reports the Fe^{3+} -selective chemodosimeter **75**, showing selective fluorescence enhancement at 440 nm ($\lambda_{\text{exc}} = 390$ nm) in DMSO/ H_2O ($v/v = 9/1$, buffered with HEPES, pH = 7.4) [84]. The probe **75** shows nanomolar detection limit of 75.7 nM for Fe^{3+} . The probe **75** shows good cell-membrane permeability, and also the Fe^{3+} -directed hydrolysis of imine linkage is shown to be detected in live HeLa cells by fluorescence microscopy. Recently [85], the probe **76** is introduced for the selective detection of Fe^{3+} in MeOH/ H_2O (9/1, v/v). The weakly emissive probe **76** shows gradual fluorescence enhancement at 430 nm upon successive incremental addition of Fe^{3+} due to the back-formation of 2,5-dimethoxybenzaldehyde and 1-aminopyrene. The probe **76** shows the LOD of 0.118 μM without any interference from other tested metal ions. Similar to the other chemodosimeters, probe **76** has been successfully applied to detect intracellular Fe^{3+} ions in live RAW264.7 cells by fluorescence microscopy. Adopting the hydrolytic cleavage of imine linkage, the multi-analytes selective chemodosimeter **77** has been developed for the detection of trivalent metal ions (Fe^{3+} , Cr^{3+} , and Al^{3+}) in THF- H_2O (8:2) medium [86]. The strong Lewis acidity of trivalent cations ($\text{Fe}^{3+}/\text{Al}^{3+}/\text{Cr}^{3+}$) selectively breaks the imine linkage, resulting in significant fluorescence enhancement at 430 nm ($\lambda_{\text{exc}} = 330$ nm). With the probe, the concentration of selective cations Fe^{3+} , Al^{3+} , and Cr^{3+} can be detected down to 0.38 nM, 0.38 nM, and 0.36 nM, respectively. Further, the probe has been applied to image the native cellular iron pools in *Candida albicans* cells.



5. Conclusions

Because of the quenching effects of Fe^{3+} , the designing of fluorescent turn-on and ratiometric probes are very challenging, and, therefore, we observed during the literature search that the majority of the reported fluorescent probes for Fe^{3+} are based on fluorescence quenching process. However, by applying the sensing mechanisms like the complexation-induced opening of the spirocyclic ring, PET, FRET, TBET, AIEE, excimer formation, etc., several Fe^{3+} -selective fluorescent turn-on and ratiometric probes have been reported after 2012. This critical review presents a total of 77 Fe^{3+} -selective fluorescent turn-on and ratiometric probes that can monitor Fe^{3+} ions, both in solution as well as within live cells. The analytical parameters like selectivity, specificity, and sensitivity of the summarized probes are suitable for their potential applications in monitoring Fe^{3+} ions concentration in various real environmental and biological samples. We believe the advantages of fluorescent probes like low-cost and simplicity would encourage the real applications of the probes summarized in this review. However, despite several analytical advantages, further research is required to develop probes that function in a pure aqueous medium because the use of organic solvents can limit their use in biological samples. Therefore, there is a wide-open scope for further research to develop novel Fe^{3+} -selective fluorescent probes with potential analytical applications.

Author Contributions: Conceptualization, S.K.S. and G.C.; methodology, S.K.S.; software, S.K.S.; validation, S.K.S.; formal analysis, S.K.S.; investigation, S.K.S.; resources, S.K.S.; data curation, S.K.S.; writing—original draft preparation, S.K.S. and G.C.; writing—review and editing, S.K.S. and G.C.; visualization, S.K.S.; supervision, S.K.S.; project administration, S.K.S.

Funding: This research received no external funding.

Conflicts of Interest: The authors declare no conflict of interest.

References

1. Abbaspour, N.; Hurrell, R.; Kelishadi, R. Review on iron and its importance for human health. *J. Res. Med. Sci.* **2014**, *19*, 164–174. [[PubMed](#)]
2. Harigae, H. Iron metabolism and related diseases: An overview. *Int. J. Hematol.* **2018**, *107*, 5–6. [[CrossRef](#)] [[PubMed](#)]
3. VanderMeulen, H.; Sholzberg, M. Iron deficiency and anemia in patients with inherited bleeding disorders. *Transfus. Apher. Sci.* **2018**, *57*, 735–738. [[CrossRef](#)] [[PubMed](#)]
4. Crisponi, G.; Nurchi, V.M.; Lachowicz, J.I. Iron Chelation for Iron Overload in Thalassemia. In *(Rditpr), Essential Metals in Medicine: Therapeutic Use and Toxicity of Metal ions in the Clinic*; De Gruyter: Boston, MA, USA; Berlin, Germany.
5. Kaur, N.; Chopra, S.; Singh, G.; Raj, P.; Bhasin, A.; Sahoo, S.K.; Kuwar, A.; Singh, N. Chemosensors for biogenic amines and biothiols. *J. Mater. Chem. B* **2018**, *6*, 4872–4902. [[CrossRef](#)]
6. Sahoo, S.K.; Kim, G.-D.; Choi, H.-J. Optical sensing of anions using C_{3v}-symmetric tripodal receptors. *J. Photochem. Photobiol. C Photochem. Rev.* **2016**, *27*, 30–53. [[CrossRef](#)]
7. Sahoo, S.K.; Sharma, D.; Bera, R.K.; Crisponi, G.; Callan, J.F. Iron(III) selective molecular and supramolecular fluorescent probes. *Chem. Soc. Rev.* **2012**, *41*, 7195. [[CrossRef](#)] [[PubMed](#)]
8. Sharma, D.; Kuba, A.; Thomas, R.; Kumar, R.; Choi, H.-J.; Sahoo, S.K. An aqueous friendly chemosensor derived from vitamin B6 cofactor for colorimetric sensing of Cu²⁺ and fluorescent turn-off sensing of Fe³⁺. *Spectrochim. Acta A* **2016**, *153*, 393–396. [[CrossRef](#)] [[PubMed](#)]
9. Sahoo, S.K.; Sharma, D.; Moirangthem, A.; Kuba, A.; Thomas, R.; Kumar, R.; Kuwar, A.; Choi, H.-J.; Basu, A. Pyridoxal derived chemosensor for chromogenic sensing of Cu²⁺ and fluorogenic sensing of Fe³⁺ in semi-aqueous medium. *J. Lumin.* **2016**, *172*, 297–303. [[CrossRef](#)]
10. Na Kim, H.; Lee, M.H.; Kim, H.J.; Kim, J.S.; Yoon, J. A new trend in rhodamine-based chemosensors: application of spirolactam ring-opening to sensing ions. *Chem. Soc. Rev.* **2008**, *37*, 1465–1472. [[CrossRef](#)]
11. Wei, Y.; Aydin, Z.; Zhang, Y.; Liu, Z.; Guo, M. A turn-on fluorescent sensor for imaging labile Fe³⁺ in live neuronal cells at subcellular resolution. *ChemBiochem* **2012**, *13*, 1569–1573. [[CrossRef](#)]

12. Chereddy, N.R.; Thennarasu, S.; Mandal, A.B. Incorporation of triazole into a quinoline-rhodamine conjugate imparts iron(III) selective complexation permitting detection at nanomolar levels. *Dalton Trans.* **2012**, *41*, 11753–11759. [[CrossRef](#)] [[PubMed](#)]
13. Huang, L.; Hou, F.; Cheng, J.; Xi, P.; Chen, F.; Bai, D.; Zeng, Z. Selective off-on fluorescent chemosensor for detection of Fe³⁺ ions in aqueous media. *Org. Biomol. Chem.* **2012**, *10*, 9634–9638. [[CrossRef](#)] [[PubMed](#)]
14. Liu, S.-R.; Wu, S.-P. New water-soluble highly selective fluorescent chemosensor for Fe (III) ions and its application to living cell imaging. *Sens. Actuators B Chem.* **2012**, *171*, 1110–1116. [[CrossRef](#)]
15. Bordini, J.; Calandreli, I.; Silva, G.O.; Ferreira, K.Q.; Leitão-Mazzi, D.P.; Espreafico, E.M.; Tfouni, E. A rhodamine-B-based turn-on fluorescent sensor for biological iron(III). *Inorg. Chem. Commun.* **2013**, *35*, 255–259. [[CrossRef](#)]
16. Saleem, M.; Abdullah, R.; Ali, A.; Park, B.J.; Choi, E.H.; Hong, I.S.; Lee, K.H. Facile synthesis, cytotoxicity and bioimaging of Fe³⁺ selective fluorescent chemosensor. *Bioorg. Med. Chem.* **2014**, *22*, 2045–2051. [[CrossRef](#)]
17. Bao, X.; Shi, J.; Nie, X.; Zhou, B.; Wang, X.; Zhang, L.; Liao, H.; Pang, T. A new Rhodamine B-based 'on-off' chemical sensor with high selectivity and sensitivity toward Fe³⁺ and its imaging in living cells. *Bioorg. Med. Chem.* **2014**, *22*, 4826–4835. [[CrossRef](#)]
18. Ji, S.; Meng, X.; Ye, W.; Feng, Y.; Sheng, H.; Cai, Y.; Liu, J.; Zhu, X.; Guo, Q. A rhodamine-based "turn-on" fluorescent probe for Fe³⁺ in aqueous solution. *Dalton Trans.* **2014**, *43*, 1583–1588. [[CrossRef](#)]
19. Sivaraman, G.; Sathiyaraja, V.; Chellappa, D. Turn-on fluorogenic and chromogenic detection of Fe(III) and its application in living cell imaging. *J. Lumin.* **2014**, *145*, 480–485. [[CrossRef](#)]
20. Sheng, H.; Meng, X.; Ye, W.; Feng, Y.; Sheng, H.; Wang, X.; Guo, Q. A water-soluble fluorescent probe for Fe(III): Improved selectivity over Cr(III). *Sens. Actuators B Chem.* **2014**, *195*, 534–539. [[CrossRef](#)]
21. Meng, W.-F.; Yang, M.-P.; Li, B.; Cheng, Z.; Yang, B.-Q. Fe³⁺-selective naked-eye 'off-on' fluorescent probe: its crystal structure and imaging in living cells. *Tetrahedron* **2014**, *70*, 8577–8581. [[CrossRef](#)]
22. Ma, S.; Yang, Z.; She, M.; Sun, W.; Yin, B.; Liu, P.; Zhang, S.; Li, J. Design and synthesis of functionalized rhodamine based probes for specific intracellular fluorescence imaging of Fe³⁺. *Dye. Pigment.* **2015**, *115*, 120–126. [[CrossRef](#)]
23. Bao, X.; Cao, X.; Nie, X.; Xu, Y.; Guo, W.; Zhou, B.; Zhang, L.; Liao, H.; Pang, T. A new selective fluorescent chemical sensor for Fe³⁺ based on rhodamine B and a 1,4,7,10-tetraoxa-13-azacyclopentadecane conjugate and its imaging in living cells. *Sens. Actuators B Chem.* **2015**, *208*, 54–66. [[CrossRef](#)]
24. Yan, F.; Zheng, T.; Shi, D.; Zou, Y.; Wang, Y.; Fu, M.; Chen, L.; Fu, W. Rhodamine-aminopyridine based fluorescent sensors for Fe³⁺ in water: Synthesis, quantum chemical interpretation and living cell application. *Sens. Actuators B Chem.* **2015**, *215*, 598–606. [[CrossRef](#)]
25. Fan, S.; Yang, W.; Hao, J.; Li, H.; Zhao, W.; Zhang, J.; Hu, Y. Cascade OFF-ON-OFF fluorescent probe: Dual detection of Fe³⁺ ions and thiols. *J. Photochem. Photobiol. A Chem.* **2016**, *328*, 129–135. [[CrossRef](#)]
26. Liu, Y.; Xu, Z.; Wang, J.; Zhang, D.; Ye, Y.; Zhao, Y. rhodamine-based "turn-on" fluorescent probe for Fe³⁺ in aqueous solution and its application in bioimaging. *Monatsh. Chem.* **2016**, *147*, 311–317. [[CrossRef](#)]
27. Chan, S.; Li, Q.; Tse, H.; Lee, A.W.M.; Mak, N.K.; Lung, H.L.; Chan, W.-H. A rhodamine-based "off-on" fluorescent chemosensor for selective detection of Fe³⁺ in aqueous media and its application in bioimaging. *RSC Adv.* **2016**, *6*, 74389–74393. [[CrossRef](#)]
28. Fan, C.; Huang, X.; Han, L.; Lu, Z.; Wang, Z.; Yi, Y. Novel colorimetric and fluorescent off-on enantiomers with high selectivity for Fe³⁺ imaging in living cells. *Sens. Actuators B Chem.* **2016**, *224*, 592–599. [[CrossRef](#)]
29. Liu, Y.; Zhang, J.; Ru, J.; Yao, X.; Yang, Y.; Li, X.; Tang, X.; Zhang, G.; Liu, W. A naked-eye visible and turn-on fluorescence probe for Fe³⁺ and its bioimaging application in living cells. *Sens. Actuators B Chem.* **2016**, *237*, 501–508. [[CrossRef](#)]
30. Gao, Y.; Liu, H.; Liu, Q.; Wang, W. A novel colorimetric and OFF-ON fluorescent chemosensor based on fluorescein derivative for the detection of Fe³⁺ in aqueous solution and living cells. *Tetrahedron Lett.* **2016**, *57*, 1852–1855. [[CrossRef](#)]
31. Wang, K.P.; Chen, J.P.; Zhang, S.J.; Lei, Y.; Zhong, H.; Chen, S.; Zhou, X.H.; Hu, Z.Q. Thiophene-based rhodamine as selective fluorescence probe for Fe(III) and Al(III) in living cells. *Anal. Bioanal. Chem.* **2017**, *409*, 5547–5554. [[CrossRef](#)] [[PubMed](#)]
32. Kumar, A.; Kumari, C.; Sain, D.; Hira, S.K.; Manna, P.P.; Dey, S. Synthesis of Rhodamine-Based Chemosensor for Fe³⁺ Selective Detection with off-on Mechanism and its Biological Application in DL-Tumor Cells. *ChemistrySelect* **2017**, *2*, 2969–2974. [[CrossRef](#)]

33. Gao, Y.; Liu, H.; Liu, Q.; Wang, W. A novel turn-on colorimetric and fluorescent sensor for Fe³⁺ and its application in living cells. *J. Photochem. Photobiol. A Chem.* **2017**, *332*, 351–356.
34. Alam, R.; Bhowmick, R.; Islam, A.S.M.; Chaudhuri, K.; Ali, M. A rhodamine based fluorescent trivalent sensor (Fe³⁺, Al³⁺, Cr³⁺) with potential applications for live cell imaging and combinational logic circuits and memory devices. *New J. Chem.* **2017**, *41*, 8359–8369. [[CrossRef](#)]
35. Wang, Y.; Chang, H.Q.; Wu, W.N.; Zhao, X.L.; Yang, Y.; Xu, Z.Q.; Xu, Z.H.; Jia, L. Rhodamine-2-thioxoquinazolin-4-one conjugate: A highly sensitive and selective chemosensor for Fe³⁺ ions and crystal structures of its Ag(I) and Hg(II) complexes. *Sens. Actuators B Chem.* **2017**, *239*, 60–68. [[CrossRef](#)]
36. Wang, K.P.; Lei, Y.; Zhang, S.J.; Zheng, W.J.; Chen, J.P.; Chen, S.; Zhang, Q.; Zhang, Y.B.; Hu, Z.Q. Fluorescent probe for Fe(III) with high selectivity and its application in living cells. *Sens. Actuators B Chem.* **2017**, *252*, 1140–1145. [[CrossRef](#)]
37. Chen, H.; Bao, X.; Shu, H.; Zhou, B.; Ye, R.; Zhu, J. Synthesis and evaluation of a novel rhodamine B-based 'off-on' fluorescent chemosensor for the selective determination of Fe³⁺ ions. *Sens. Actuators B Chem.* **2017**, *242*, 921–931. [[CrossRef](#)]
38. Jin, X.; Wang, S.; Yin, W.; Xu, T.; Jiang, Y.; Liao, Q.; Xia, X.; Liu, J. A highly sensitive and selective fluorescence chemosensor for Fe³⁺ based on rhodamine and its application in vivo imaging. *Sens. Actuators B Chem.* **2017**, *247*, 461–468. [[CrossRef](#)]
39. Zhou, T.; Chen, X.; Hua, Q.; Lei, W.; Hao, Q.; Zhou, B.; Su, C.; Bao, X. Synthesis and evaluation of a new furfuran-based rhodamine B fluorescent chemosensor for selective detection of Fe³⁺ and its application in living-cell imaging. *Sens. Actuators B Chem.* **2017**, *253*, 292–301. [[CrossRef](#)]
40. Ozdemir, M.; Zhang, Y.; Guo, M. A highly selective "off-on" fluorescent sensor for subcellular visualization of labile iron(III) in living cells. *Inorg. Chem. Commun.* **2018**, *90*, 73–77. [[CrossRef](#)]
41. Wang, L.; Li, W.; Zhi, W.; Wang, Y.; Han, J.; Cao, Z.; Ni, L.; Li, H.; Jing, J. A water-soluble Fe³⁺ selective fluorescent turn-on chemosensor: Preparation, theoretical study and its optical vitro imaging. *J. Lumin.* **2018**, *196*, 379–386. [[CrossRef](#)]
42. Wang, J.; Long, L.; Xiao, G.; Fang, F. Reversible Fluorescent Turn-on Sensors for Fe³⁺ based on a Receptor Composed of Tri-oxygen Atoms of Amide Groups in Water. *Open Chem.* **2018**, *16*, 1268–1274. [[CrossRef](#)]
43. Murugan, A.S.; Vidhyalakshmi, N.; Ramesh, U.; Annaraj, J. In vivo bio-imaging studies of highly selective, sensitive rhodamine based fluorescent chemosensor for the detection of Cu²⁺/Fe³⁺ ions. *Sens. Actuators B Chem.* **2018**, *274*, 22–29. [[CrossRef](#)]
44. Wang, Y.; Song, F.; Zhu, J.; Zhang, Y.; Du, L.; Kan, C. Highly selective fluorescent probe based on a rhodamine B and furan-2-carbonyl chloride conjugate for detection of Fe³⁺ in cells. *Tetrahedron Lett.* **2018**, *59*, 3756–3762. [[CrossRef](#)]
45. Song, F.; Yang, C.; Liu, H.; Gao, Z.; Zhu, J.; Bao, X.; Kan, C. Dual-binding pyridine and rhodamine B conjugate derivatives as fluorescent chemosensors for ferric ions in aqueous media and living cells. *Analyst* **2019**, *144*, 3094–3102. [[CrossRef](#)] [[PubMed](#)]
46. Cao, X.; Zhang, F.; Bai, Y.; Ding, X.; Sun, W. A Highly Selective 'Turn-on' Fluorescent Probe for Detection of Fe³⁺ in Cells. *J. Fluores.* **2019**, *29*, 425–434. [[CrossRef](#)]
47. Gao, Z.; Kan, C.; Liu, H.; Zhu, J.; Bao, X. A highly sensitive and selective fluorescent probe for Fe³⁺ containing two rhodamine B and thiocarbonyl moieties and its application to live cell imaging. *Tetrahedron* **2019**, *75*, 1223–1230. [[CrossRef](#)]
48. Sui, B.; Tang, S.; Liu, T.; Kim, B.; Belfield, K.D. Novel BODIPY-Based Fluorescence Turn-on Sensor for Fe³⁺ and Its Bioimaging Application in Living Cells. *ACS Appl. Mater. Interfaces* **2014**, *6*, 18408–18412. [[CrossRef](#)]
49. Pathak, R.K.; Dessingou, J.; Hinge, V.K.; Thawari, A.G.; Basu, S.K.; Rao, C.P. Quinoline Driven Fluorescence Turn On 1,3-Bis-calix [4]arene Conjugate-Based Receptor to Discriminate Fe³⁺ from Fe²⁺. *Anal. Chem.* **2013**, *85*, 3707–3714. [[CrossRef](#)]
50. Nandre, J.; Patil, S.; Patil, V.; Yu, F.; Chen, L.; Sahoo, S.; Prior, T.; Redshaw, C.; Mahulikar, P.; Patil, U. A novel fluorescent "turn-on" chemosensor for nanomolar detection of Fe(III) from aqueous solution and its application in living cells imaging. *Biosens. Bioelectron.* **2014**, *61*, 612–617. [[CrossRef](#)]
51. Yang, X.; Liu, X.; Li, Y.; Wu, F.; Mao, J.; Yuan, Y.; Cui, Y.; Sun, G.; Zhang, G. A differentially selective probe based on diketopyrrolopyrrole with fluorescence turn-on response to Fe³⁺, and dual-mode turn-on and ratiometric response to Au³⁺ and its application in living cell imaging. *Biosens. Bioelectron.* **2016**, *80*, 288–293. [[CrossRef](#)]

52. Qiu, L.; Zhu, C.; Chen, H.; Hu, M.; He, W.; Guo, Z. A turn-on fluorescent Fe³⁺ sensor derived from an anthracene-bearing bisdiene macrocycle and its intracellular imaging application. *Chem. Commun.* **2014**, *50*, 4631–4634. [[CrossRef](#)] [[PubMed](#)]
53. Pandith, A.; Choi, J.H.; Jung, O.S.; Kim, H.S. A simple and robust PET-based anthracene-appended O-N-O chelate for sequential recognition of Fe³⁺/CN⁻ ions in aqueous media and its multimodal applications. *Inorg. Chim. Acta* **2018**, *482*, 669–680. [[CrossRef](#)]
54. Lim, B.; Baek, B.; Jang, K.; Lee, N.K.; Lee, J.H.; Lee, Y.; Kim, J.; Park, J.; Kim, S.; Kang, N.W.; et al. Novel turn-on fluorescent biosensors for selective detection of cellular Fe³⁺ in lysosomes: Thiophene as a selectivity-tuning handle for Fe³⁺ sensors. *Dye. Pigment.* **2019**, *169*, 51–59. [[CrossRef](#)]
55. Simon, T.; Shellaiah, M.; Srinivasadesikan, V.; Lin, C.C.; Ko, F.H.; Sun, K.W.; Lin, M.C. A simple pyrene based AIEE active Schiff base probe for selective naked eye and fluorescence off-on detection of trivalent cations with live cell application. *Sens. Actuators B Chem.* **2016**, *231*, 18–29. [[CrossRef](#)]
56. Chung, P.K.; Liu, S.R.; Wang, H.F.; Wu, S.P. A Pyrene-based Highly Selective Turn-on Fluorescent Chemosensor for Iron(III) Ions and its Application in Living Cell Imaging. *J. Fluoresc.* **2013**, *23*, 1139–1145. [[CrossRef](#)] [[PubMed](#)]
57. Han, C.; Huang, T.; Liu, Q.; Xu, H.; Zhuang, Y.; Li, J.; Hu, J.; Wang, A.; Xu, K. Design and synthesis of a highly sensitive “Turn-On” fluorescent organic nanoprobe for iron(iii) detection and imaging. *J. Mater. Chem. C* **2014**, *2*, 9077–9082. [[CrossRef](#)]
58. Dwivedi, S.K.; Gupta, R.C.; Ali, R.; Razi, S.S.; Hira, S.K.; Manna, P.P.; Misra, A. Smart PET based organic scaffold exhibiting bright “Turn-On” green fluorescence to detect Fe³⁺ ion: Live cell imaging and logic implication. *J. Photochem. Photobiol. A Chem.* **2018**, *358*, 157–166. [[CrossRef](#)]
59. Kundu, B.K.; Singh, R.; Tiwari, R.; Nayak, D.; Mukhopadhyay, S. Amide probe as selective Al³⁺ and Fe³⁺ sensor inside the HeLa, and A549 cell lines: Pictet-Spengler reaction for rapid detection of tryptophan amino acid. *New J. Chem.* **2019**, *43*, 4867–4877. [[CrossRef](#)]
60. Kim, N.H.; Lee, J.; Park, S.; Jung, J.; Kim, D. A Schiff Base Fluorescence Enhancement Probe for Fe(III) and Its Sensing Applications in Cancer Cells. *Sensors* **2019**, *19*, 2500. [[CrossRef](#)] [[PubMed](#)]
61. Nandhini, T.; Kaleeswaran, P.; Pitchumani, K. A highly selective, sensitive and “turn-on” fluorescent sensor for the paramagnetic Fe³⁺ ion. *Sens. Actuators B Chem.* **2016**, *230*, 199–205. [[CrossRef](#)]
62. Erdemir, S.; Kocyigit, O. Anthracene excimer-based “turn on” fluorescent sensor for Cr³⁺ and Fe³⁺ ions: Its application to living cells. *Talanta* **2016**, *58*, 63–69. [[CrossRef](#)] [[PubMed](#)]
63. Lee, M.H.; Kim, J.S.; Sessler, J.L. Small molecule-based ratiometric fluorescence probes for cations, anions, and biomolecules. *Chem. Soc. Rev.* **2015**, *44*, 4185–4191. [[CrossRef](#)] [[PubMed](#)]
64. Chereddy, N.R.; Thennarasu, S.; Mandal, A.B. A highly selective and efficient single molecular FRET based sensor for ratiometric detection of Fe³⁺ ions. *Analyst* **2013**, *138*, 1334–1337. [[CrossRef](#)] [[PubMed](#)]
65. Chereddy, N.R.; Nagaraju, P.; Raju, M.N.; Krishnaswamy, V.R.; Korrapati, P.S.; Bangal, P.R.; Rao, V.J. A novel FRET ‘off-on’ fluorescent probe for the selective detection of Fe³⁺, Al³⁺ and Cr³⁺ ions: Its ultrafast energy transfer kinetics and application in live cell imaging. *Biosens. Bioelectron.* **2015**, *68*, 749–756. [[CrossRef](#)] [[PubMed](#)]
66. Lohar, S.; Banerjee, A.; Sahana, A.; Banik, A.; Mukhopadhyay, S.K.; Das, D. A rhodamine–naphthalene conjugate as a FRET based sensor for Cr³⁺ and Fe³⁺ with cell staining application. *Anal. Methods* **2013**, *5*, 442–445. [[CrossRef](#)]
67. Wu, Y.-X.; Li, J.-B.; Liang, L.-H.; Lu, D.-Q.; Zhang, J.; Mao, G.-J.; Zhou, L.-Y.; Zhang, X.-B.; Tan, W.; Shen, G.-L.; et al. A rhodamine-appended water-soluble conjugated polymer: an efficient ratiometric fluorescence sensing platform for intracellular metal-ion probing. *Chem. Commun.* **2014**, *50*, 2040–2042. [[CrossRef](#)] [[PubMed](#)]
68. Chen, W.D.; Gong, W.T.; Ye, Z.Q.; Lin, Y.; Ning, G.L. FRET-based ratiometric fluorescent probes for selective Fe³⁺ sensing and their applications in mitochondria. *Dalton Trans.* **2013**, *42*, 10093–10096. [[CrossRef](#)] [[PubMed](#)]
69. Xie, P.; Guo, F.; Xia, R.; Wang, Y.; Yao, D.; Yang, G.; Xie, L. A rhodamine–dansyl conjugate as a FRET based sensor for Fe³⁺ in the red spectral region. *J. Lumin.* **2014**, *145*, 849–854. [[CrossRef](#)]
70. Wang, C.; Liu, Y.; Cheng, J.; Song, J.; Zhao, Y.; Ye, Y. Efficient FRET-based fluorescent ratiometric chemosensors for Fe³⁺ and its application in living cells. *J. Lumin.* **2015**, *157*, 143–148. [[CrossRef](#)]

71. Das, S.; Aich, K.; Goswami, S.; Quah, C.K.; Fun, H.K. FRET-based fluorescence ratiometric and colorimetric sensor to discriminate Fe³⁺ from Fe²⁺. *New J. Chem.* **2016**, *40*, 6414–6420. [[CrossRef](#)]
72. Qin, J.C.; Yang, Z.Y.; Wang, G.Q.; Li, C.R. FRET-based rhodamine–coumarin conjugate as a Fe³⁺ selective ratiometric fluorescent sensor in aqueous media. *Tetrahedron Lett.* **2015**, *56*, 5024–5029. [[CrossRef](#)]
73. Wang, C.; Zhang, D.; Huang, X.; Ding, P.; Wang, Z.; Zhao, Y.; Ye, Y. A fluorescence ratiometric chemosensor for Fe³⁺ based on TBET and its application in living cells. *Talanta* **2014**, *128*, 69–74. [[CrossRef](#)] [[PubMed](#)]
74. Sen, S.; Sarkar, S.; Chattopadhyay, B.; Moirangthem, A.; Basu, A.; Dhara, K.; Chattopadhyay, P. A ratiometric fluorescent chemosensor for iron: discrimination of Fe²⁺ and Fe³⁺ and living cell application. *Analyst* **2012**, *137*, 3335–3342. [[CrossRef](#)] [[PubMed](#)]
75. Ghosh, K.; Tarafdar, D. Piperazine-based new sensor: selective ratiometric sensing of Fe³⁺, logic gate construction and cell imaging. *Supramol. Chem.* **2015**, *27*, 224–232. [[CrossRef](#)]
76. Wang, M.; Wang, J.; Xue, W.; Wu, A. A benzimidazole-based ratiometric fluorescent sensor for Cr³⁺ and Fe³⁺ in aqueous solution. *Dye. Pigment.* **2013**, *97*, 475–480. [[CrossRef](#)]
77. Wang, Y.; Yang, M.-Y.; Zheng, M.-H.; Zhao, X.-L.; Xie, Y.-Z.; Jin, J.-Y. 2-Pyridylthiazole derivative as ICT-based ratiometric fluorescent sensor for Fe(III). *Tetrahedron Lett.* **2016**, *57*, 2399–2402. [[CrossRef](#)]
78. Kuwar, A.; Patil, R.; Singh, A.; Sahoo, S.K.; Marek, J.; Singh, N. A two-in-one dual channel chemosensor for Fe³⁺ and Cu²⁺ with nanomolar detection mimicking the IMPLICATION logic gate. *J. Mater. Chem. C* **2015**, *3*, 453–460. [[CrossRef](#)]
79. Du, J.; Hu, M.; Fan, J.; Peng, X. Fluorescent chemodosimeters using “mild” chemical events for the detection of small anions and cations in biological and environmental media. *Chem. Soc. Rev.* **2012**, *41*, 4511. [[CrossRef](#)]
80. Wang, R.; Yu, F.; Liu, P.; Chen, L. A turn-on fluorescent probe based on hydroxylamine oxidation for detecting ferric ion selectively in living cells. *Chem. Commun.* **2012**, *48*, 5310–5312. [[CrossRef](#)]
81. Long, L.; Zhou, L.; Wang, L.; Meng, S.; Gong, A.; Zhang, C. A ratiometric fluorescent probe for iron(III) and its application for detection of iron(III) in human blood serum. *Anal. Chim. Acta* **2014**, *812*, 145–151. [[CrossRef](#)]
82. Upadhyay, Y.; Anand, T.; Babu, L.T.; Paira, P.; SK, A.K.; Kumar, R.; Sahoo, S.K. Combined use of spectrophotometer and smartphone for the optical detection of Fe³⁺ using a vitamin B6 cofactor conjugated pyrene derivative and its application in live cells imaging. *J. Photochem. Photobiol. A Chem.* **2018**, *361*, 34–40. [[CrossRef](#)]
83. Chen, Y.-Z.; Bhorge, Y.R.; Pape, A.J.; Divate, R.D.; Chung, Y.-C.; Yen, Y.-P. A New Schiff Base Chemodosimeter for Fluorescent Imaging of Ferric Ions in Living Cells. *J. Fluoresc.* **2015**, *25*, 1331–1337. [[CrossRef](#)]
84. Tsai, H.-T.; Bhorge, Y.R.; Pape, A.J.; Janaki, S.N.; Yen, Y.-P. A Selective Colorimetric and Fluorescent Chemodosimeter for Fe(III) Ion Based on Hydrolysis of Schiff Base. *J. Chin. Chem. Soc.* **2015**, *62*, 316–320. [[CrossRef](#)]
85. Chiang, Y.-K.; Bhorge, Y.R.; Divate, R.D.; Chung, Y.-C.; Yen, Y.-P. A New Schiff Base Chemodosimeter: Selective Colorimetric and Fluorescent Detection of Fe (III) Ion. *J. Fluoresc.* **2016**, *26*, 1699–1708. [[CrossRef](#)]
86. Venkateswarulu, M.; Mukherjee, T.; Mukherjee, S.; Koner, R.R. Turn-on trivalent cation selective chemodosimetric probe to image native cellular iron pools. *Dalton Trans.* **2014**, *43*, 5269. [[CrossRef](#)]

